Complexity Measures of Electroencephalographic Data

PIERRE-ALAIN MARZIO

MSc by Research in Pattern Analysis and Neural Network

Supervisor: Professor David Lowe

ASTON UNIVERSITY

September 1999

ASTON UNIVERSITY

Complexity Measures of Electroencephalographic Data

PIERRE-ALAIN MARZIO

MSc by Research in Pattern Analysis and Neural Network, 1999

Thesis Summary

The intention of this project is to examine whether it is possible to measure alertness using EEG recorded on awake subjects. This thesis tries to examine if a measure of attentiveness could be derived from measures of complexity of EEG data.

In order to avoid averaging required by Fourier analysis, a dynamical embedding is realised. As well, it allows us to reconstruct and to characterise the underlying generator of the data. On the results of this embedding, a signal filtering is proposed and different measures of complexity are derived. An analysis of these measures is performed by comparing them with information available about the attentiveness of the subject during the experiments.

Finally, a feature extraction is performed. On the basis of this feature extraction, a filtering of the signal is realised. It may allows us to improve the accuracy of the different measures proposed.

Keywords: EEG, Dynamical Embedding, Principal Component Analysis, Singular Value Decomposition, Complexity, Independent Component Analysis

Acknowledgements

First, I would like to thank my supervisor, Professor David Lowe, for his help, advice and useful comments during this nine months project. I would thank him for the ability to always find time to answer to my questions.

I would also like to thank British Aerospace and Doctor Helen Stone of Sowerby Research Centre for the general background about the data.

Finally I am grateful to my parents and all my friends on Aston Campus for their support and the pleasant atmosphere throughout the academic year, in particular the MSc and PhD students of the NCRG.

Contents

1 Introduction **7**

2 Brain waves and EEG data **10**
- 2.1 Electroencephalography 10
- 2.2 Brain waves 12
- 2.3 Data and experiment 14

3 Embedding Approach **19**
- 3.1 Dynamical embedding 20
  - 3.1.1 Dynamical systems and the method of delays 20
  - 3.1.2 Embedding space decomposition 22
- 3.2 Characterisation of the window size 23
  - 3.2.1 A toy example 24
  - 3.2.2 Using the EEG data 26
- 3.3 Determining the number of delay vectors 28

4 Measures of complexity **31**
- 4.1 Introduction 31
- 4.2 Determining the complexity 32
  - 4.2.1 Characterisation of the complexity 32
  - 4.2.2 Visual inspection of complexity 33
  - 4.2.3 Simple measures of complexity 35
- 4.3 Entropy Measure 38
  - 4.3.1 Definition and comments 38
  - 4.3.2 Results 38
  - 4.3.3 Improvements 40
- 4.4 Fisher's Information based measure 42
  - 4.4.1 Definition 42
  - 4.4.2 Results 43
- 4.5 Angular Measure 45
- 4.6 Discussion 45

5 Feature Extraction **50**
- 5.1 Independent Component Analysis 50
- 5.2 Independent Component Analysis on the EEG data 51
- 5.3 Results 54
  - 5.3.1 Results with entropy 55

5.3.2 Results with Fisher 55
5.4 Discussion 56

6 Conclusions **58**

A Analysis of the video tape **63**
A.1 Trial 2: 12:00-12:59 64
A.2 Trial 3: 13:47-14:47 65
A.3 Trial 4: 15:10-16:11 67

B Comparisons between channels **69**
B.1 Comparisons in the choice of the parameters of the embeddings 69
B.2 Simple measures of complexity 72
B.3 Entropy measure applied to other channels 73
B.4 Fisher based measure applied to other channels 75

List of Figures

2.1 Recording of electroencephalographic data 11
2.2 The four kind of brain waves 13
2.3 Electrodes placement 17

3.1 Noiseless sine wave 25
3.2 Noisy sine wave 26
3.3 Sine wave with poor signal to noise ratio 27
3.4 Effects of the number of delays on the EEG singular values 29
3.5 Error function for the EEG 29
3.6 Effects of the number of delays on the EEG singular values 30

4.1 Number of significant singular values determined using the scree test . 34
4.2 Simple measures of complexity 37
4.3 Entropy measure on channel O1 39
4.4 Spectrum of singular values of channel O1 40
4.5 Restricted entropy measure on channel O1 41
4.6 Fisher's information based measure applied on channel O1 43
4.7 Restricted Fisher's information based measure 44
4.8 Angular measure applied to channel O1 46

5.1 Independent sources 52
5.2 Entropy measure after ICA decomposition 55
5.3 Fisher's Information based measure after ICA decomposition 56

B.1 Convergence of stretched spectra and error for channel O2 70
B.2 Convergence of stretched spectra and error for channel P4 70
B.3 Convergence of stretched spectra and error for channel FZ 71
B.4 Convergence of stretched spectra and error for channel C3 71
B.5 Measures of complexity 72
B.6 Entropy measures for channel O2 73
B.7 Entropy measures for channel P4 74
B.8 Fisher's Information based measures for channel O2 75
B.9 Fisher's Information based measures for channel P4 76

Chapter 1

Introduction

Among the different techniques used to investigate brain activity, the most used method is without any doubt the recording of the electric potentials on the scalp. This technique is known as electroencephalography (EEG). Since its first development by Berger in 1928, EEG has been widely used as a clinical tool for the diagnosis of brain diseases, and used as a non-invasive approach for research in the quantitative study of human neurophysiology.

EEG and brain states

Correlation between human behaviours and changes in the spectrum of the EEG was noted first by Lomis et al. in 1937 when they observed that the EEG spectrum mostly shifts towards lower frequencies at transition to sleep. The link between the changes in the EEG spectrum and the behavioral states of the mind is strong enough that the EEG spectra can be used to discriminate alert and asleep states.

If several mental states can be distinguish using only the EEG spectra, we can then ask if it is possible to estimate the vigilance and the attentiveness of a subject using only the EEG record. Several studies of alertness have confirmed that despite sincere intentions, few people remain vigilant while engaged in monotonous monitoring tasks [12], [11].

The most common approach to study electroencephalograms is *Fourier Analysis* with the study of the power and coherence spectra. The main reason why the EEG are studied in the frequency domain is the belief of the linear nature of the biological phenomena recorded by the EEG. This method supposes that EEG could then be described in term of sinusoidal components.

Fourier Analysis and frequency analysis require an averaging of the time series to compute the Fourier transformations. In order to avoid this averaging and to consider shorter segments of time series, we can use the embedding approach. The strength of this method is that it allows us to reconstruct the manifold and to study the dynamical properties of a system without any knowledge about the original manifold.

The first intention of this project was to examine whether it is possible to derive a measure of attentiveness from human electroencephalograms obtained from wake, normal individuals. In this thesis, we do not propose a measure of vigilance but we rather inspect several measures of complexity and we inspect the link between the changes in these measures and the behaviour of the subject.

Complexity measures

When visually inspecting signals, one of the first impressions they give is that some of them seem to vary more than others. It could then be interesting to characterise the complexity and richness of these signals. The measure of the complexity can then be used as an intuitive description of signals. More, it allows us to compare signals recorded in different conditions, such as a set of patients in a biomedical area.

Many different methods have been proposed to attempt to quantify signal complexity. Some of them are not suited to analysis of biological signals because they are variant in the presence of noise or non-stationarities [15].

Several measures were investigated with electroencephalograms, such as Optimal Model Order under regressive modelling, Spectral Entropy and Approximate Entropy, and measures based on the Embedding-space Decomposition [14]. Because there is no absolute definition of complexity, each of these methods measures different features of the signal. For example spectral entropy measures the spectral entropy of the signal using the Fourier Transformations when Optimal Model Order measures the number of past samples required to predict the time series in a autoregressive model.

From these methods, the embedding-space decomposition give better results, so the presented measures are based on the singular values resulting from this decomposition.

Plan of the thesis

The first chapter is this introduction.

The second chapter gives a brief presentation of electroencephalography. It presents the biological phenomena which generate the electrical potentials recorded and describes the common brain waves observed in wake subjects. Finally, the data used in this thesis are presented.

The third chapter is an introduction to the embedding approach used in this work, Taken's delay coordinate maps. It gives also a description of the embedding-space decomposition method. At the end of the chapter the methods used to choose the parameters of the embedding are presented.

In chapter 4, different measures are proposed and discussed. The correlation with their changes and the behaviour of the subject is also discussed.

In chapter 5, a feature extraction is performed on the data using the Independent Component Analysis (ICA). The results of this decomposition are discussed and some measures proposed in chapter 4 are applied on selected independent sources.

Chapter 6 concludes this thesis and discusses the major results.

Chapter 2

Brain waves and EEG data

Introduction

The human brain can be studied in many different ways. Several methods allow us to measure physical processes inside living tissues. These methods include positron emission tomography (PET), magnetic resonance imaging (MRI), electroencephalography (EEG) or magnetoencephalography (MEG). They differ by temporal and spatial resolutions and by the physical process recorded. PET records chemical consumption of oxygen and glucose by the neurons when MEG and EEG record electrical activity of the brain. The temporal resolutions can vary in a range of minutes for PET and milliseconds for EEG and MEG [13].

Each method has its own region of applicability. Nevertheless, the oldest method (and probably the cheapest one), the electroencephalography, has been used for years in the study of human behaviour.

2.1 Electroencephalography

Electroencephalography (EEG) is a medical imaging technique that measures brain function by analyzing the scalp electrical activity generated by brain structures. It is a completely noninvasive and painless procedure that can be applied repeatedly in patients, normal adults, and children with no risks or limitations.

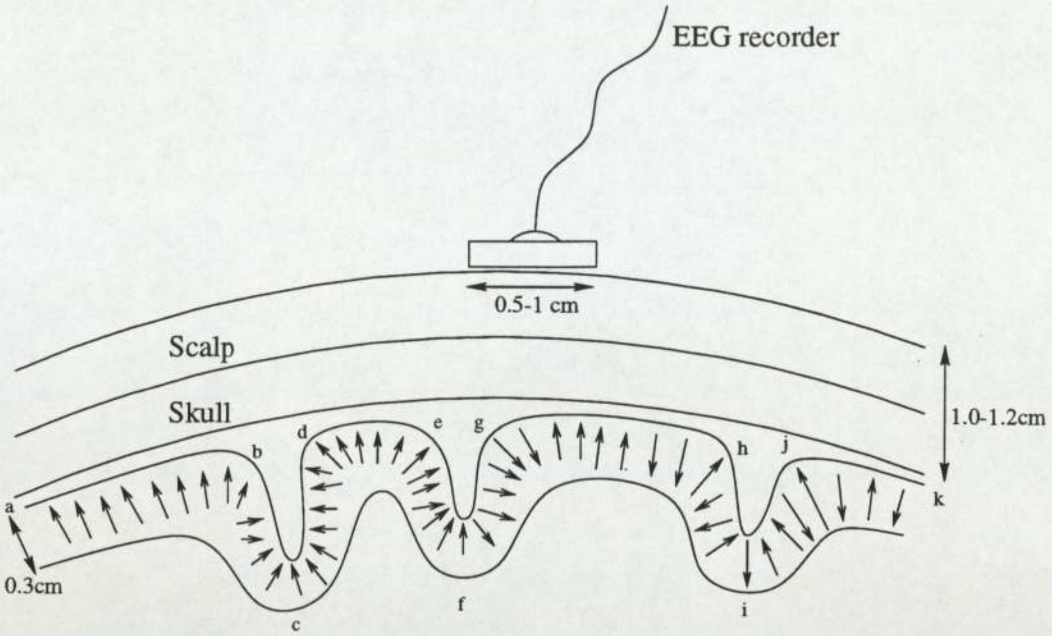

Figure 2.1: Extracranial recording of electroencephalographic data

For these reasons, electroencephalography has been used for years in the diagnosis of a large variety of brain diseases, the most common of which are epilepsy (a brain disorder usually not accompanied by any abnormalities detectable with nonfunctional imaging techniques), sleep disorders, stroke, head trauma, encephalopathies, Alzheimer's disease, etc. For the same reasons, it has been widely used to study brain organisation of cognitive processes such as perception, memory, attention, language, and emotion in normal adults and children.

The spatial resolution of EEG is limited about to 10 cm^2 [13]. The reasons are the size of the sensors and the diffusion caused by tissue conductivity of the skull and the scalp. Due to the technique used, the EEG are more sensitive to the sources present in the neocortex rather than deep sources in the brain. The sources (shown as arrows on figure 2.1) are the macrocolumns of the neocortex. A macrocolumn is a macrostructure of the brain which contains about 10^6 neurons and about 10^{10} synapses. The EEG are more sensitive to correlated fields perpendicular to the surface of the scalp (as in regions a–b or d–e) than correlated tangential fields in the sculcus as in region e–g. Finally, EEG is completely insensitive to opposing dipoles in sculcus (b–d).

2.2 Brain waves

Interpreting EEG involves the characterisation of waves usually defined by their frequencies and their morphologies.

The raw EEG is usually described in terms of frequency bands. The frequencies of the human EEG waves vary between about 0.5 Hz and 50 Hz (we can assume that all signals with frequencies greater than 50 Hz are simply noise because no physiological mechanisms can produce such signals). This range has been divided in four main bands which are known as *alpha, beta, theta* and *delta* waves.

- **Alpha activity**

  Alpha waves are the EEG waves with frequencies between 7 and 13 Hz. They are strongest over the occipital cortex (posterior region of the head) and also over frontal cortex. α-activity is brought out by closing the eyes and by relaxation, and abolished by eye opening or alerting by any mechanism (thinking, calculating). Alpha has been linked to extraversion (introverts show less), creativity (creative subjects show alpha when listening and coming to a solution for creative problems), and mental work. It is the major rhythm seen in normal relaxed adults - it is present during most of life especially beyond the thirteenth year when it dominates the resting tracing.

- **Beta activity**

  Beta activity is 'fast' activity. It has a frequency of 13 Hz and greater. It is usually seen on both sides in a symmetrical distribution and is most evident frontally. It is the normal rhythm when we have our eyes open and are listening and thinking. It reflects desynchronised active brain tissues. It is the dominant rhythm in patients who are alert or anxious.

- **Theta activity**

  Theta activity has a frequency of 3.5 to 7.5 Hz and is classed as 'slow' activity. It is abnormal in awake adults but is perfectly normal in children up to 13 years and in the first stages of sleep. It can be seen as a focal disturbance in focal subcortical lesions and in generalized distribution in diffuse disorders.

- **Delta activity**

  Delta activity is 3 Hz or below. It tends to be the highest in amplitude and the slowest waves. It is quite normal and is the dominant rhythm in infants up to one year and in stages 3 and 4 of sleep. It may occur focally with subcortical lesions and in general distribution with diffuse lesions, metabolic encephalopathy hydrocephalus or deep midline lesions. It is usually most prominent frontally in adults and posteriorly in children.

Sometimes, the terms of gamma or mu activity are used. The gamma band corresponds to signals with frequencies greater than 30 Hz. Often, the gamma activity is included in the beta band. The mu activity is the beta activity recorded in a particular area of the scalp.

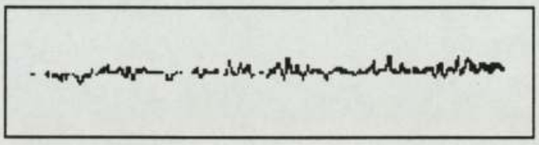

(a) Alpha rhythm

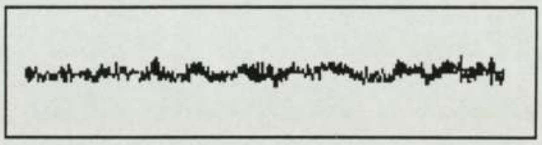

(b) Beta rhythm

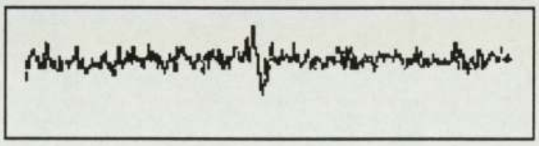

(c) Theta rhythm

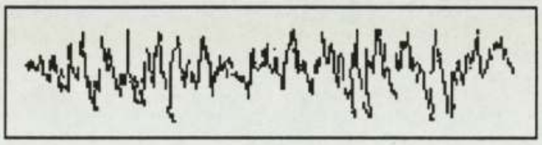

(d) Delta rhythm

Figure 2.2: **The four kinds of brain waves**

Another way to describe EEG waves is to define their morphology. Certain waves have characteristic forms irrespective of their frequency and are recognisable by their shape: in other instances pairs or groups of waves have typical appearances. Single waves that are specially shaped include, for instance spikes or sharp waves - waves that rise rapidly to a point and fall away equally dramatically with a base that is small compared to the wave's amplitude.

The difficulty in EEG reading lies in recognising the artifacts and also in being able to differentiate normal variants from abnormalities.

The normal variants are waves or patterns of waves which are unusual in appearance but which are not significant for abnormalities or diseases. These waves can be misinterpreted. The artifacts are disturbances in EEG, caused by technical defects such as electrode movements with loss of contact, scratching the scalp, sweating, etc or by natural human activity, muscular activity obscuring the EEG, eyes movements, etc.

2.3 Data and experiment

The data used in this thesis was provided by Dr Helen Stone of British Aerospace (Sowerby). The data collected on awake subjects who were monitored continuously from 10 am to 5 pm during a series of four tasks and including normal rest and lunch breaks. The subjects for this experiment are people from both genders and handedness. A timetable was drawn up to ensure that all subjects carried out their tasks at similar time-of-day to allow comparison between them. In this thesis we only use data collected on a righthanded female (referenced as subject ba16kb) and no comparison between different subjects has been done.

The main goal of this study is to attempt to define a measure of alertness, so the subjects were monitored during four tracking tasks. These trials were designed to be particularly monotonous and repetitious and they consist of a mixture of three different activities:

- A tracking activity which is present in all four tasks. The subject must maintain a horizontal line which deviates vertically and horizontally under computer control.
- A response activity which requires the subject to press the first joystick button when a particular signal appears on the screen.
- Another response activity where the signal is now a number on the screen. The subject must press the second button of the joystick if the number is ± 2 equal

to the previous one.

The timetable 2.1 corresponds to activities followed by subject 16. The starting and stopping times were collected using a video recording of the experiments. Due to a problem with the sensor on channel P4, the EEG recording was stopped from 11:43 to 11:53, but strange records with this channel can be detected even earlier so the period 11:20-11:53 was excluded from the study.

The EEG data were collected on an Oxford Instruments Medilog system utilising multiple measurement channels. The electrodes were sited according to the international 10-20 system. The sampling rate used for the recording was 256 Hertz and the data was quantised to two bytes per sample.

Eighteen different channels are present in the dataset. Some of them are synchronisation information from the task program. The following channels were available:

- Bipolar C4-A1
- EOGl/FP1 and EOGr/FP2, these channels measure eyes movement activity.
- EOGinf/FPinf and EOGsup/FPsup, these channels provide information about blink activity and eyelid position.
- C3
- T3
- T4
- O1
- O2
- P4
- Cz
- Fz

Task Number	Activity	Start	Stop
1	EOG calibration	10:13	10:14
2	**Trial 1** (Tracking + event)	10:15	11:15
3	EOG calibration	11:16	11:19
4	*Refreshment break*	11:20	11:53
5	EOG calibration	11:53	11:58
6	**Trial 2** (Tracking only)	11:59	12:59
7	EOG calibration	13:00	13:01
8	*Lunch break*	13:02	13:39
9	EOG calibration	13:40	13:44
10	**Trial 3** (Tracking + number + event)	13:47	14:47
11	EOG calibration	14:48	14:52
12	*Refreshment break*	14:53	15:04
13	EOG calibration	15:05	15:09
14	**Trial 4** (Tracking + number)	15:10	16:11
15	EOG calibration	16:11	16:17
16	*Refreshment break and final debriefing*	16:18	17:00

Table 2.1: Timetable for subject 16

- EMG1 and EMG2 these locations are used to monitor muscle activity.

In the study, several channels were used in order to consider handedness and effects of the muscular activity over the measures of complexity (the region which controls the muscular activity is a frontal one).

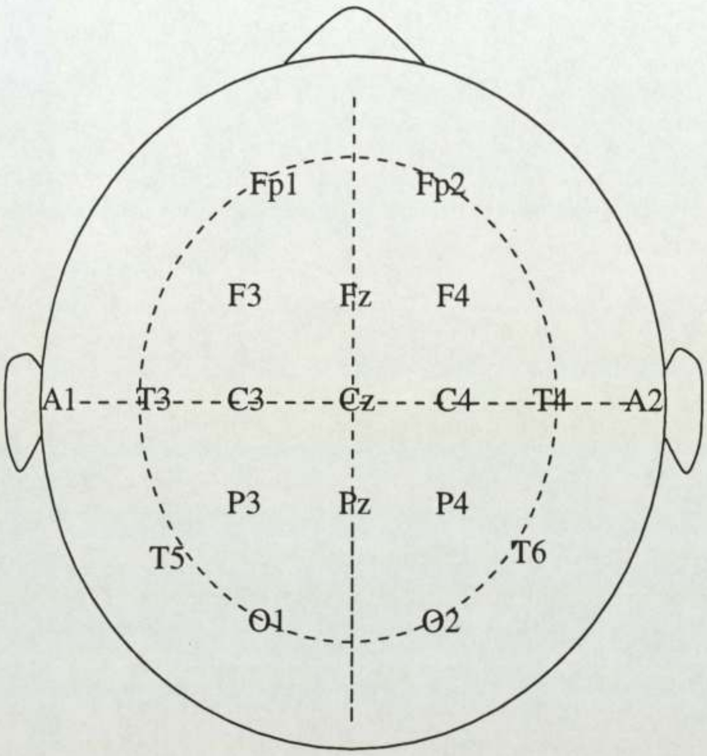

Figure 2.3: **Electrodes placement:** international 10-20 system

In addition to the EEG, a recording of the output of the task program is available. It consists of a measure of the deviation of the tracking line from the centred and horizontal position. The scaling rate for this measure was 10 hertz. This record contains also the information about the random events and the numbers shown on the screen and the corresponding responses from the observer. It allows us to compute the performance of the subject during the trials but we cannot guarantee that this performance is correlated with alertness and then that it can be used to validate our own EEG-based measures of attentiveness.

Finally, a video recording of each trial and EOG calibration is available. This video allows us to check for abnormal behaviours during the trials, for example eating, drinking, movements, etc. A list of these events for the four trials is presented in appendix A. On the basis of this video record, we chose not to use the performance recorded by the computer described in the previous paragraph because we observe no correlation between the performance and the observations we can do using the video tape. For example, around 14:30, the subject fell asleep for several minutes, with no major correlation with the performance.

Chapter 3

Embedding Approach

Introduction

Several methods can be applied to EEG analysis. Traditional approaches rely upon averaging long segments of time series and performing Fourier analysis to examine the resulting power and coherency spectra. The main reason why EEG data are studied in the frequency domain is the belief of the linear nature of the biological phenomena recorded by the electroencephalograms. This method suggests that the signals could be decomposed in a sum of sinusoidal components. The signals could then be described in term of their harmonics. Several studies of alertness use this approach [12], [11] and claim that the EEG spectrum and vigilance are correlated.

In this thesis, we use another method, the embedding approach, which allows us to consider shorter segments of time series. Also, it allows us to reconstruct the underlying generator of the time series and then to consider the parameters of this generator. Another interest of the embedding approach consists in the possibility to perform a temporal analysis of the EEG channels instead of a spatial analysis: usually, the different channels from the different regions of the scalp are considered and a Principal Component Analysis (PCA) or Independent Component Analysis (ICA) is performed on the resulting data. Using the embedding approach, we can compute a PCA or an ICA on the data from a single channel: we only consider the data from the embedding space instead of the raw EEG. For these different reasons, we chose to use the embedding theory instead of time analysis using Fourier Transforms. The embedding theory will be described in the following sections.

First, this chapter discusses the embedding approach applied to analysis of electroencephalographic data and in the last two sections, the methods used to choose the parameters of the embedding are presented.

3.1 Dynamical embedding

3.1.1 Dynamical systems and the method of delays

Consider a continuous system governed by the set of N first-order differential equations

$$\frac{dX_i\,(t)}{dt} = F_i(X_1, X_2, \ldots, X_N, t)\,, \qquad i = 1, \ldots, N \tag{3.1}$$

where the F_i are non-linear functions of the independent variables X_i. Each $X(t) = (X_1, \ldots, X_N, t)$ represents the state of the system at time t and may be thought as a point in a vector space S. The dimensionality of S, since it controls the number of possible states, will be associated with the degrees of freedom of the system.

Often, as the system evolves, the set of vectors $X(t)$ could be contained in a subspace D of the space S and the flow of points will contract onto sets of lower dimensions than the dimension of S. These sets are called *attractors* and the knowledge of their description is useful to describe the system itself. An important measure of the dynamics of a system is its complexity, which is related to the dimension of the subspace containing the attractors.

We wish now to use the same principle to measure the complexity of the EEG data. The theorem which allows us to reconstruct the unknown dynamical system was demonstrated by Takens [18] and the method of delays we use was introduced first by Broomhead and King [2]. The vocabulary used in the following sections is the vocabulary introduced by these authors.

The method of delays consists in projecting the time series samples x_t in a vector space, the embedding space. In this space, the data are represented by the embedding vectors $X(t)$ defined by

$$X(t) = \begin{bmatrix} x_t \\ x_{t-\tau} \\ \vdots \\ x_{t-(M-1)\tau} \end{bmatrix} \tag{3.2}$$

where τ represents the time increment or lag and M is the embedding size. The lag τ is chosen as a multiple of the sampling time τ_s. With our data, the sampling frequency is 256 Hz, so the sampling time is $\tau_s = 1/256$. According to [2], we choose τ to be equal to τ_s so we use all the samples from the EEG records. This choice allows us to assimilate the singular value decomposition to a PCA of the initial data [2].

There is no absolute criterion to choose the second parameter M. We only know that the window size M must be greater than $2*D+1$ where D represents the dimension of the manifold (condition required by the proof of Taken's theorem [18]). The method we adopt for the study is explained in section 3.2.

Consider now the sequence of vectors $X(t) = X_1, X(t+\tau) = X_2, X(t+2\tau) = X_3, \ldots, X(t+(n+1)\tau) = X_n$. Each of these vectors will represent a point in the embedding space $\mathbb{R}^M$. The sequence will then draw the discrete trajectory of the data. Let us define $\mathbf{X}$ to be the trajectory matrix.

$$\mathbf{X} = \frac{1}{\sqrt{N}}[X_1, X_2, X_3, \ldots, X_n] = \frac{1}{\sqrt{N}} \begin{bmatrix} x_t & x_{t+\tau} & \cdots & x_{t+n\tau} \\ x_{t+\tau} & x_{t+2\tau} & \cdots & x_{t+(n+1)\tau} \\ \vdots & \vdots & & \vdots \\ x_{t+(M-1)\tau} & x_{t+M\tau} & \cdots & x_{t+(M+n-1)\tau} \end{bmatrix} \tag{3.3}$$

where $\frac{1}{\sqrt{N}}$ has been introduced as a convenient normalisation [2].

We want to characterise this trajectory, and if possible measure the dimension of the subspace containing the attractors. It was shown that the analysis of the complexity of the trajectory matrix leads to the singular values decomposition problem.

3.1.2 Embedding space decomposition

Consider the real (and not square) matrix $\mathbf{X}$, we may decompose it as

$$\mathbf{X} = U * S * V^T \tag{3.4}$$

In this decomposition, the matrix S is diagonal. Let σ_i be the diagonal elements of S, then σ_i^2 is the i^{th} eigenvalue of $\mathbf{C} = \mathbf{X} * \mathbf{X}^T$. We also know that $\sigma_i \geq 0$. The columns of the matrix V are the eigenvectors of $\mathbf{C}$ and the matrix U is the matrix of projections of $\mathbf{X}$ onto the eigenvectors of $\mathbf{C}$. This decomposition is usually referred to as the singular value decomposition.

When we constructed the trajectory matrix $\mathbf{X}$, we know that the window size must respect the inequality

$$M \geq 2 * D + 1 \tag{3.5}$$

Since D is not known a priori, this means that in practice the embedding dimension M is chosen large enough such that redundancy appears in the embedding results. This redundancy manifests itself as a rank deficiency in the embedding matrix $\mathbf{X}$. We may decompose the trajectory matrix using equation 3.4 to investigate this redundancy.

For noiseless systems, some σ_i are zero and the number of non-zero singular values is the dimension of the manifold. Real systems (and EEG data in particular) are always corrupted by noise, noise from the recording process, quantisation noise, etc. The trajectory will then explore all the dimensions of the embedding space. This results in a spreading out of the cloud of embedding vectors in the embedding space around the manifold. The result on the singular spectrum is a shifting of the singular values. If the noise is randomly distributed, there is no preferred direction in the embedding space and the noise appears as a noise-floor in the singular spectrum.

If we are able to identify the noise floor in the singular values spectrum, we can then determine the dimension of the manifold. Moreover, it allows us to partition the embedding space in two parts, the first one where the signal is dominant and the second one where the noise is the dominant feature. If we suppose we can split the set of singular values in two parts, a signal set and a noise one, we can then define the projection operators on the two corresponding subspaces. Using the notation of the equation 3.4, the projection operator on the signal subspace will be made up of the columns of V corresponding to the singular values above the noise floor. In the same way, the matrix U is the projection of the embedding matrix $\mathbf{X}$ on the eigenvectors of $\mathbf{X} * \mathbf{X}^T$, so the projection of the embedding vectors are the corresponding rows of the matrix U.

This decomposition of the embedding space corresponds to a PCA on the embedding vectors, because the singular values σ_i are the square root of the eigenvalues of the covariance matrix $\mathbf{X} * \mathbf{X}^T$. It can be used to enhance the signal to noise ratio, but ICA methods have been proposed to perform feature extraction on EEG data with better results [7], [6] and [8]). The ICA method will then be used in the last part of this thesis to enhance the signal to noise ratio, but singular value decomposition will be used to characterise the manifold using the singular values.

3.2 Characterisation of the window size

In the previous sections, we haven't chosen any value for the window size. Finding such a window size is a very subjective problem. Takens, in his proof of his theorem shows that M must respect the inequality 3.5. Usually, M is chosen large enough to respect this inequality. A too large window size will introduce a lot of redundancy in the embedding. In this section, we wish to find a "good" value for this value which respects the inequality in order to capture the whole dynamics in the embedding, but not too big in order to decrease as much as possible the computation time and the computation complexity.

Some of the measures presented in this thesis are based on the computation of the singular values. To allow comparison between measures at different times of the day, we must choose a window size which respects the inequality for the different periods of the day. We must also try to reduce the influence of the window size on the singular values.

3.2.1 A toy example

In order to present the method developed for the choice of M, a simple toy example is used. Consider the following mixture of sinusoidal components:

$$\begin{aligned} f(t) \;=\; & \sin(20\pi t) \;+\; 0.9 * \sin(58\pi t) \;+\; \ldots \\ & \cos(22\pi t) \;+\; 1.1 * \cos(36\pi t) \;+\; \alpha \,*\, \eta_t \end{aligned} \tag{3.6}$$

Where η_t is a Gaussian noise source of unit variance. From this equation we generate 3000 points with 256 points per second. The frequencies of these sine waves correspond to frequencies observed in EEG signal. We then apply the method of delays as described previously and we compute the singular values for different values of M between 5 and 100 by step of 5.

The figure 3.1 presents the results of noiseless data i.e. $\alpha = 0$. The dimension of the manifold is clearly equal to eight. In the embedding space, each sinusoid has two degrees of freedom: the curve defined by the points $(x_t, x_{t+1}, \ldots, x_{t+M-1})$ is an ellipse if the samples are generated from one sinusoid, a four-dimensional ellipsoid for two sinusoid and an eight-dimensional ellipsoid for our example.

With this example, we see that a lag greater than 10 is useless (after 8 the singular values are zero), but on the graph, it becomes obvious only for a lag greater than 20. This example is unrealistic because no noise corrupted the signal so we consider now a noisy signal.

The next figure (3.2) is the same figure but with some noise (α set to 1). As said before, due to the presence of noise the trajectory will explore all the dimension of the embedding space. On the spectra of the singular values, the noise is visible as the noise floor present in figure 3.2(b). The level of this floor depends of the level of noise in the toy signal: increasing α will raise the floor.

Here, The choice of a correct embedding dimension could be determined by the observation of a "convergence of the spectra". With this example, the convergence is

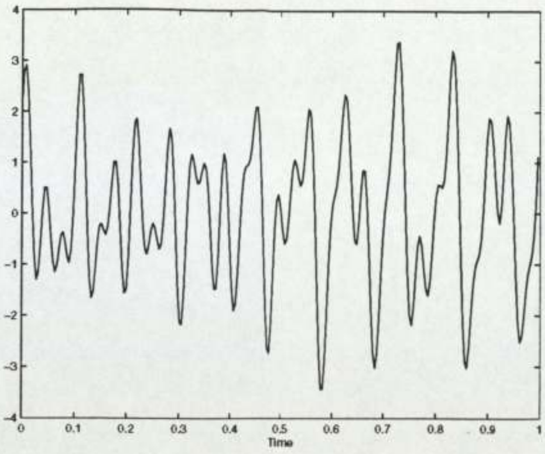

(a) Noiseless data sequence

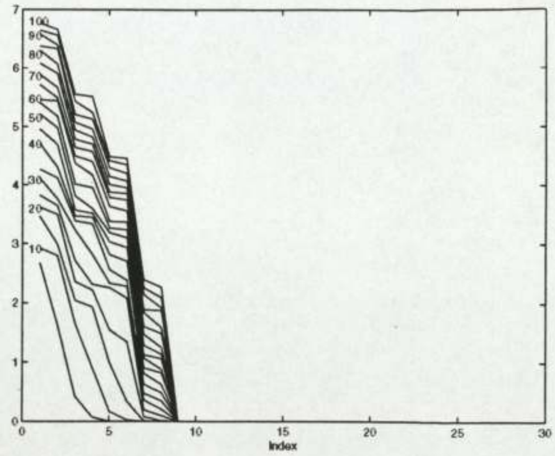

(b) Spectra of singular values

Figure 3.1: **Noiseless sine wave example:** (a) Noiseless data sequence used in the construction of the delay vectors (b) Effect of variation of the windows size on the spectra of singular values, the numbers correspond to the window sizes of the different spectra.

observed for $M \geq 40$. With EEG data, this criterion cannot be applied strictly because the convergence of the spectra of the singular values is not visible.

As a last example, the same function (described in equation 3.6) is used but with a poor signal to noise ratio (now α is set to be equal to 3). As shown in figure 3.3, the signal is now highly corrupted (a). As an effect of this corruption, the spectra now do not converge but a spread effect and a right shift of the singular values are observed (b).

If we look closer to the spectra on figure 3.3(b), we can see that the curve seems to adopt the same shape when the number of delays increase and a convergence of the shapes of the curves may be expected. Figure 3.3(c) presents the method used to see if such a convergence exists. The shortest spectra are stretched to the length of the longest one and plotted on the same graph. The method used to stretch the spectra consists of interpolating the curves with the same number of points as the longest curve, 100 in the present case.

Finally, the euclidean distance between two successive stretched spectra is used to

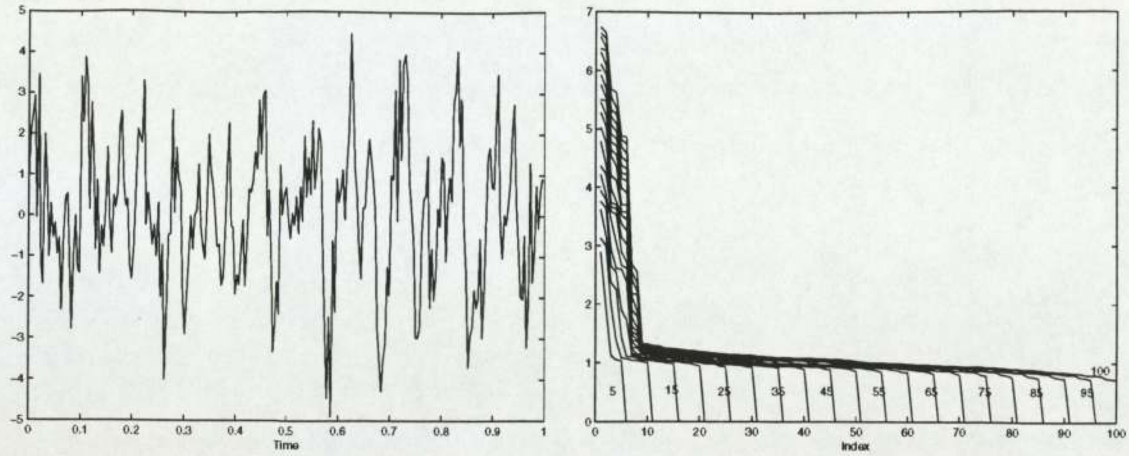

(a) Noisy signal *(b) Spectra of singular values*

Figure 3.2: **Noisy sine wave example:** (a) Noisy data sequence (b) Effect of variation of the windows size on the spectra of singular values, the numbers on the graph represent the window sizes used to compute the spectra.

characterise the convergence,

$$E(M) = \sqrt{\sum_{i=1}^{100} (\sigma_i - \sigma_i')^2} \tag{3.7}$$

where σ_i and σ_i' are the interpolated singular values for the spectra of length M and the consecutive one. This function is not really adapted to characterise convergence, but it allows us to determine the effects of the variation of the window size on the spectra. The lower values of this distance function will indicate that the variation in the number of delays will less modify the shape of the spectrum. In our case, it may be an interesting criterion for the choice of the lag. Nevertheless, using the results of figure 3.3, a correct value for M seems to be around 80 when we know that the trajectory is contained in a subspace of dimension 8 (figure 3.1). So we may expect big values for M.

3.2.2 Using the EEG data

The EEG data behave as the last example of the previous section, i.e. we observe a right shift of the singular values. An explanation can be a poor signal to noise ratio

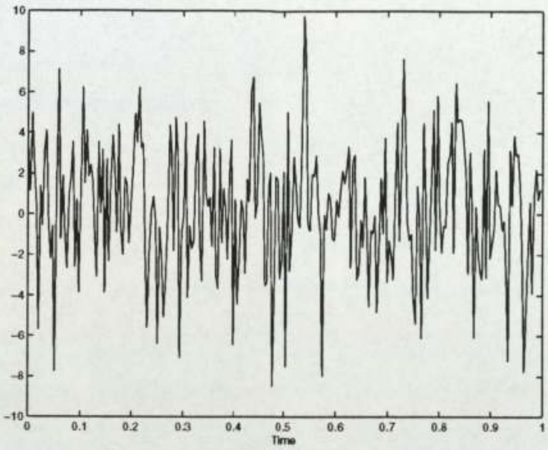

(a) Noisy signal

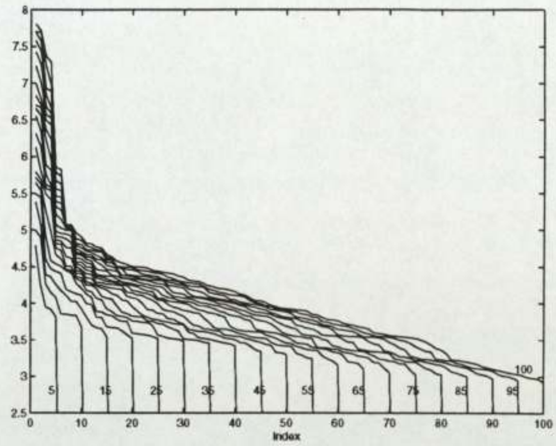

(b) Spectra of singular values

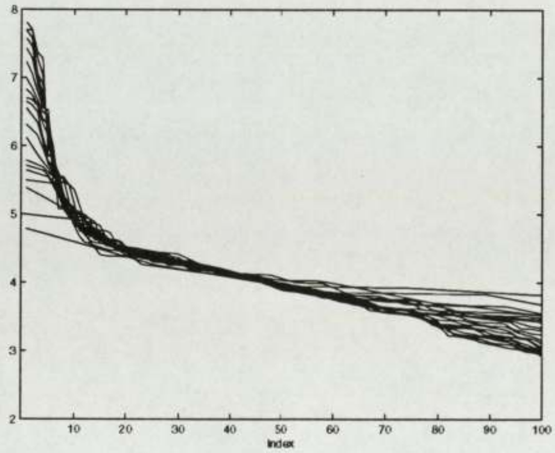

(c) Stretched spectra

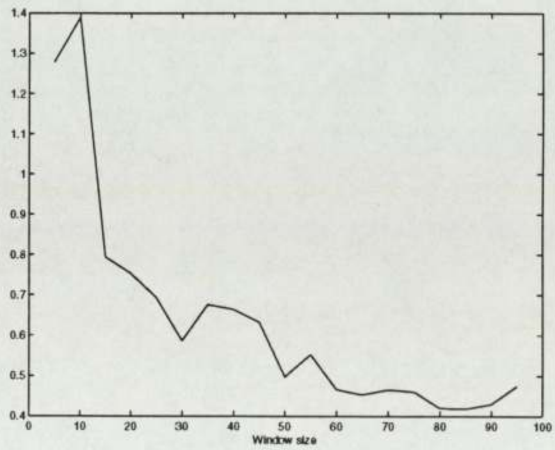

(d) Error function

Figure 3.3: **Sine wave with poor signal to noise ratio:** (a) Noisy data sequence (b) Effect of variation of the windows size, the numbers represent the window sizes of the different spectra (c) Stretched spectra (d) Quadratic error between two successive spectra.

but the presence of artifacts in the signal or the nonstationarity of the generator may also explain this effect. In the previous section, we studied the effects of noise on the singular spectra and we presented a criterion to choose the window size. The effects of nonstationarities have not been studied in this thesis and could be part of future work.

In this section, the EEG data are collected on the channel O1. The results for other channels are presented in appendix B.1.

We apply the method of delays and the singular values decomposition to an embedding matrix which represents the different periods of the day. This matrix is made up of 5000 embedding vectors chosen at different times of the trials and the breaks. So we expect to capture the different behaviours of the singular spectra and then be able to chose a value for M which will apply anytime. The figure 3.4 presents the spectra of the singular values for number of delays between 10 and 250 by step of 10.

If we use the error function defined for the sine wave example, we observe a minimum at about 150. In previous work ([8]), a window size equal to 30 was used for a sampling frequency equal to 100. If the sampling rate is doubled, we then need twice more points to capture the same period of signal so we may expect a value about 80 if the sampling rate is equal 256. We know that the criterion we used with the toy example gives to high values for M. So a value of 150 may not be a bad choice for the window size. This is the value we choose for our computation in the rest of the study.

3.3 Determining the number of delay vectors

In the previous section, we choose to use 5000 delay vectors. This choice is rather subjective. Now the lag is determined, could it be possible to reduce the number of embedding vectors ? Using a lag of 150, 5000 delay vectors represent about 20 seconds of the initial time series. A smaller number of embedding vectors will reduce the length of time series required as well as it will reduce the computation complexity and calculation time.

If the number of delay vectors is too small, the embedding matrix will be unable to capture the dynamics of the data. The results will be a change in the shape of the

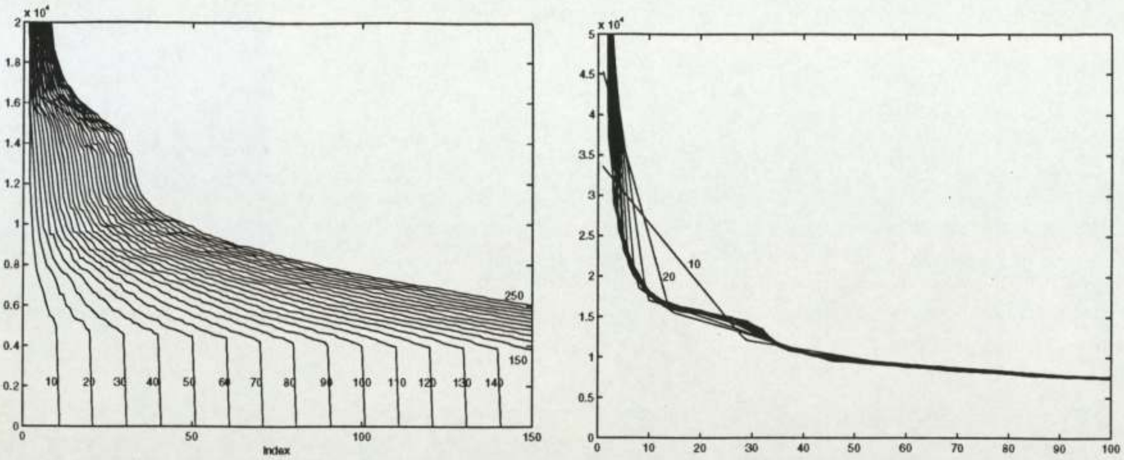

(a) Singular values *(b) Stretched spectra*

Figure 3.4: **Spectra of singular values for different window size:** (a) Spectra of singular values, the numbers are the window sizes (b) Stretched singular spectra

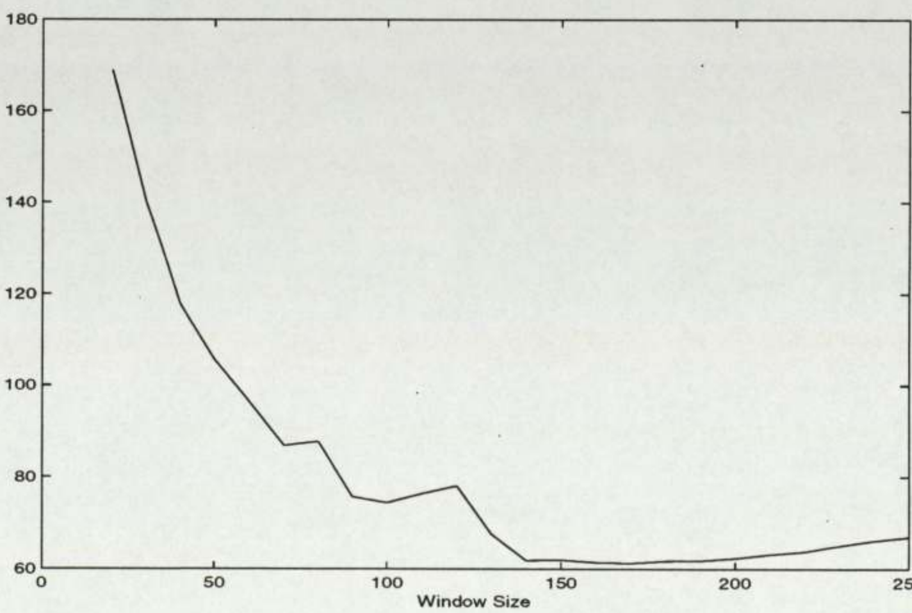

Figure 3.5: **Plot of the distance between consecutive spectra**

spectrum of the singular values. Once the embedding matrix is large enough to capture the dynamics of the time series, the addition of embedding vectors to the trajectory matrix will not modify the spectrum of the singular values. So, the criterion for a sufficient number of delay vectors could be a convergence of the spectra.

Using data from channel O1, we compute the singular value decomposition on a set of 20 trajectory matrices, with a lag of 150 but a number of delay vectors varying between 500 and 10000 by step of 500. Figure 3.6 presents the 20 spectra (a) and the plot of the error functions (b). The error function used is the euclidean distance between two successive spectra. The plot of error function tell us that 2500 delay are sufficient to observe a convergence of the spectra and then to capture the dynamics for the day. If the sampling rate is $\tau_s = 256$, 2500 embedding vectors correspond then to about 10 seconds of the time series.

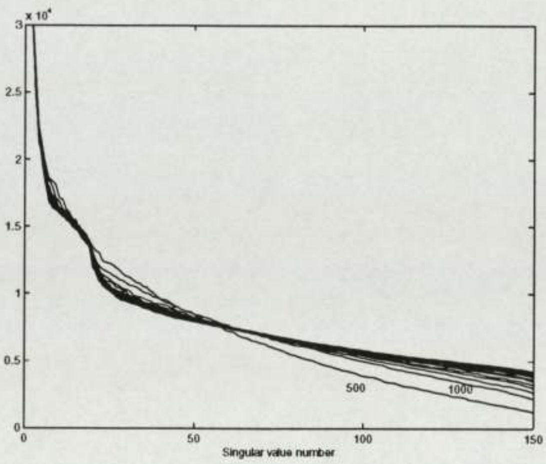

(a) Singular spectra

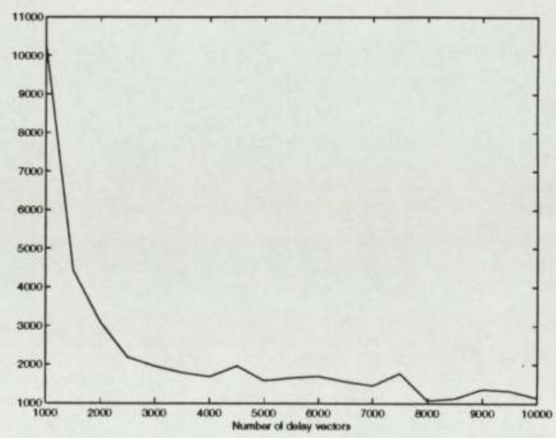

(b) Error function

Figure 3.6: **Effects of the number of delay vectors on the singular spectra**

Chapter 4

Measures of complexity

4.1 Introduction

One important piece of information about a time series is its complexity. Several measures exist to estimate the complexity of a time series. In this thesis, we apply embedding theory on the EEG data. This theory allows us to reconstruct the underlying generators of the time series in an embedding dimension $\mathbb{R}^M$. The different measures proposed in this chapter try to estimate the parameters of this manifold. They can estimate either the dimension of the subspace containing the generators or the shape of the manifold.

Embedding theory is subject to the choice of several parameters. In the following sections, the value used for the window size will be the value determined in the previous chapter ($M = 150$).

In this chapter, only data from 12:00 to 15:00 are used. We choose this period to consider only a continuous segment of recording, without any recording break inside it (there is a break in records between 11:43 and 11:53 in the data used). This period starts with the second trial and stops at the end of the recording.

Some of the proposed measures use the results of the singular value decomposition to estimate the complexity. The same procedure was used for the calculation of the singular values for each measure:

- We split the range 12:00-17:00 in sections of one minute. This duration can be reduced to sections of 10 seconds because 2500 embedding vectors capture the dynamics of the signal (previous chapter). We chose to consider sections of one minute in order to reduce the number of singular value decomposition which is quite long to compute.

- For each minute, we construct an embedding matrix as described in equation 3.3. The number of embedding vectors to construct this matrix is equal to 2500. It represents about 10 seconds of the EEG signal. In order to avoid ignoring 50 seconds of signal for each section, the embedding vectors are chosen to be uniformly spaced in the section (the embedding vectors are constructed with an overlapping equal to 144).

- We then perform a singular value decomposition on each embedding matrix. The computed singular values represent the characteristics of the embedding (the lengths of the cloud of embedding vectors in the embedding space). They are then stored and be used for the calculation of the different measures.

We may expect that in EEG time series, the complexity is related to the states of the brain, i.e. that the complexity of EEG varies with the activity realised by the subject and his concentration. The problem with this hypothesis is that the complexity may vary for a large number of different reasons and we do not know if the the effects of concentration and attentiveness can be isolated among the other sources of brain waves.

4.2 Determining the complexity

4.2.1 Characterisation of the complexity

As mentioned in the previous chapter, finding the complexity (here an upper bound of the dimension of the underlying manifold) leads to finding a noise floor in the spectrum of singular values. In the case of a signal with a good signal to noise ratio, the detection of this floor can be obvious (the second sine wave example in the previous chapter). But as the noise increases, the noise floor raises and can then reach the same level as signal.

To find the noise floor in this case, one of the most simple tests, and probably the most used is the *scree test* [3]. It derives from a visual inspection of the singular values plotted against their root number. A typical plot of singular values shows a steep slope over the first roots and a gradual trailing off for the rest of the eigenvalues (the scree). The term scree derives from the resemblance to the rubble that forms at the foot of a mountain.

The main problem with the scree test is that this criterion is rather subjective and the separation between the signal part and the noise dominated one is often not obvious. The method is then to detect the kink in the shape of the spectrum. Sometimes several kinks can be observed and may increase the difficulty of applying the method.

4.2.2 Visual inspection of complexity

To apply the scree test to our data and estimate the complexity, we compute the singular values spectra using the procedure described before. The 300 embedding decompositions are then visually analyzed to determine the number of significant values, which we take to imply complexity.

We perform this analysis on four different channels, the 2 occipital channels O1 and O2, a frontal one FZ and the channel P4 in order to see the differences between the different locations on the scalp.

The results of these inspections are shown in figure 4.1. The dashed lines in the plots represent the start and end times of breaks/trials. The stars represent the sections where inattention of the subject can be observed (group 3 and 4 of the appendix A). The plus signs and the crosses represent the events of groups 1 and 2 respectively. These events are plotted to inspect their effects on the measure.

As mentioned previously, the main problem of these inspections is that we cannot reproduce these results due to the subjectivity of the method. Nevertheless, some

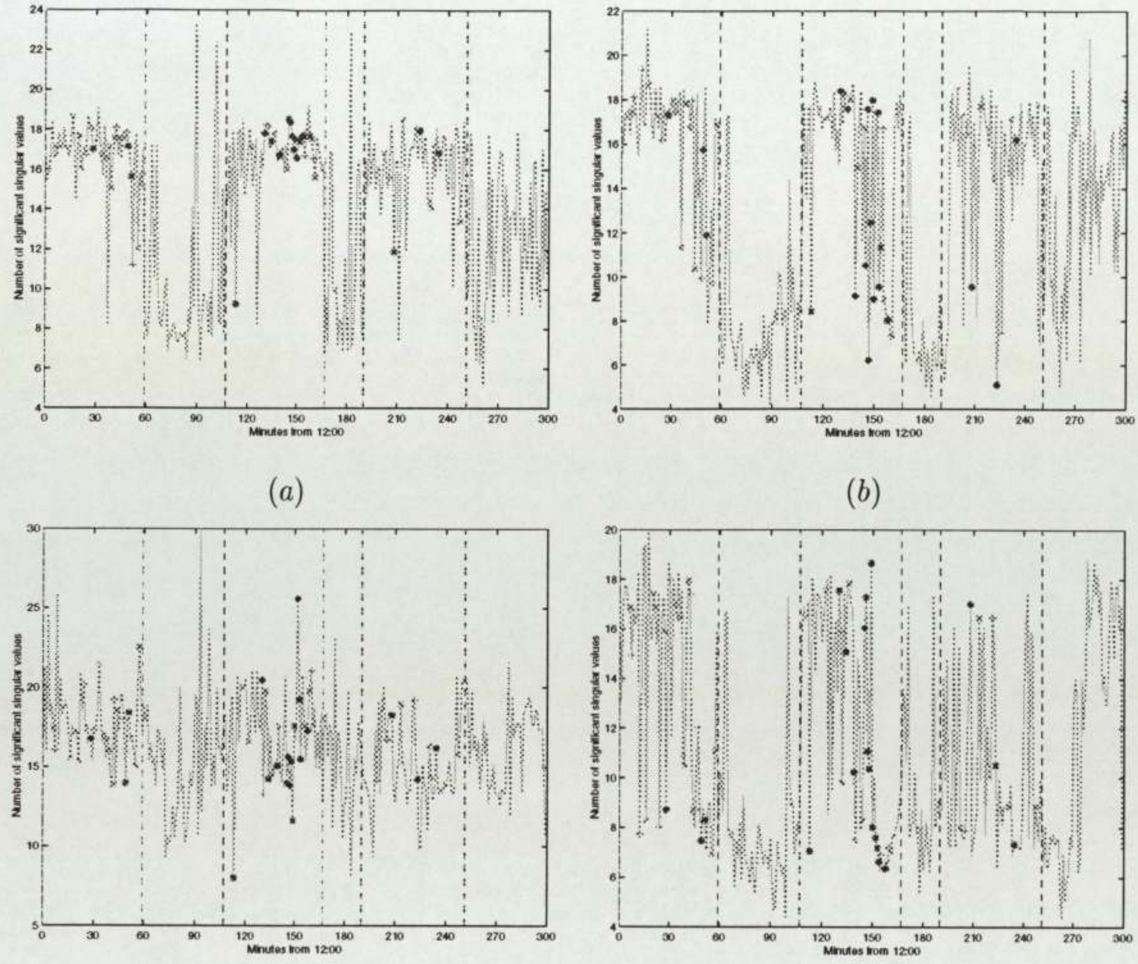

Figure 4.1: **Number of significant singular values determined using the scree test:** four EEG channels were inspected, 2 occipital ones O1 (a) and O2 (b), one frontal channel FZ (c) and the channel P4 (d).

interesting points can be observed:

- First, during the analysis of the spectra, we observed that the spectra may be split in two groups by their shapes. The first ones are more present during the periods of concentration, during the experiments. They often present an obvious kink around the 18^{th} eigenvalue. The second shape seems to characterise the periods of rest. It is characterised by higher eigenvalues and by the absence of kinks in the curve. A change in the curvature could sometimes be observed for eigenvalues near 70, but it is often too smooth to be considered.

- Strong differences can be observed between the channel FZ and the three others. An explanation could be that we observe here the effects of the muscular activity (the frontal channels are located over the regions of the cortex controlling the muscular activity [13]).

- This measure of complexity may be used to cluster the periods of activity (minutes 0-59, 107-167 and 190-250) from the breaks. The rest periods are characterised by a lower complexity than the experiment periods. Using a threshold as clustering criterion, the best separation is obtained with channel O1. We can observe also that the the number of significant singular values decreases at the end of each trials when it stays constant for channel O1. Another remark concerns the period around the minute 150 (14:30): the number of significant singular values stays constant contrary to other channels. According to the video, during this period, the subject is subject to several mini-sleep periods.

4.2.3 Simple measures of complexity

To remove the subjective analysis in the previous computation, we wish to define a measure of complexity. One simple way to do it is just to consider the percentage of variance explained by the first n dominant eigenvectors:

$$\text{Percentage of variance explained} = \frac{\sum_{j=1}^{n} \sigma'_j}{\sum_{k=1}^{M} \sigma_k} \tag{4.1}$$

Usually, this formula is used with n constant. Here we want to define a measure which gives us an estimation of the number of significant singular values. We will instead choose a percentage of variance to explain and find the number of dominant eigenvectors required to explain this variance. The definition of the measure will then be:

$$M_4(t) = n, \quad \text{with respect} \quad \frac{\sum_{i=1}^{n} \sigma_i}{\sum_{j=1}^{M} \sigma_j} = Constant \tag{4.2}$$

On the same model, we can define three other measures:

$$M_1(t) = n, \quad \text{with respect} \quad \sigma_n = Constant \tag{4.3}$$

$$M_2(t) = n, \quad \text{with respect} \quad \sum_{i=1}^{n} \sigma_i = Constant \tag{4.4}$$

$$M_3(t) = n, \quad \text{with respect} \quad \frac{\sigma_n}{\sum_{j=1}^{M} \sigma_j} = Constant \tag{4.5}$$

The results of these four measures are highly dependent on the choice of the threshold. As shown in figure 4.2, functions M_1, M_3 and M_4 give similar results. In addition, the variations of these functions are anticorrelated with the results of the scree test: the measure increases during the break periods. Only measure M_2 presents results similar to the scree test.

Once again, the measures are able to differentiate the lunch or refreshment break periods from the trials. The break periods are certainly characterised by a larger number of movements from the subject, especially during the lunch break. This suggests that our measures once again are high sensitive to artifacts.

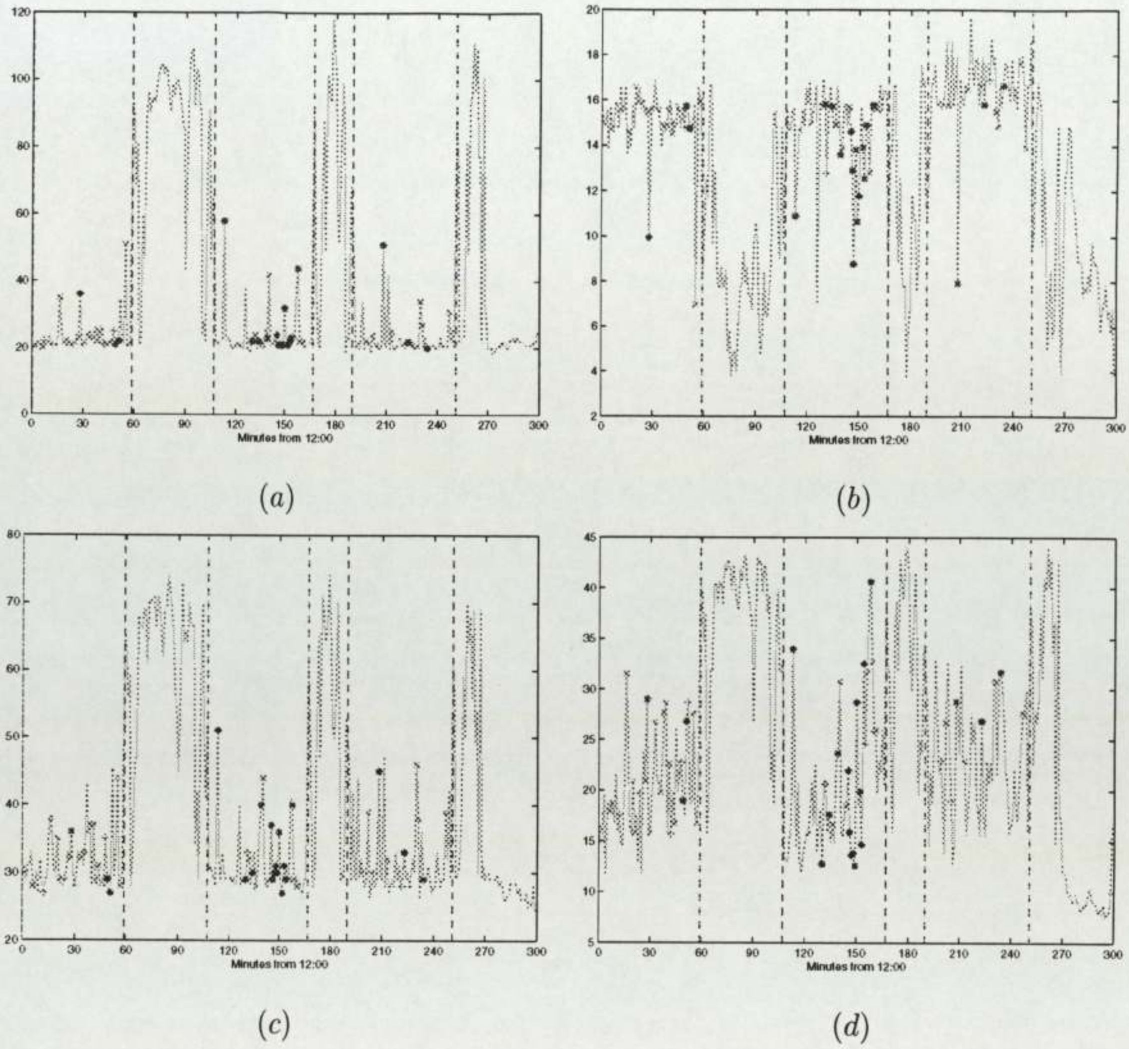

Figure 4.2: **Number of significant singular values determined using the four measures (channel O1):** (a) measure M_1 with a threshold of 2500, (b) M_2 with a threshold of 80000, (c) M_3 with a threshold of $7.5 * 10^{-3}$ and (d) M_4 with a threshold equal to 0.5.

4.3 Entropy Measure

4.3.1 Definition and comments

The concept of entropy was originally developed by physicists to discriminate order from disorder in the physical sciences, initially in thermodynamics. Entropy was introduced into information theory by Shannon in 1948. It could be interpreted as a measure of disorder or as a measure of the information content [1]. For a continuous function p with $0 < p(x) \leqslant 1$, its definition is

$$E = -\int p(x)\,\log p(x)\,dx \tag{4.6}$$

To describe and measure the variation of the spectrum of singular values, we may use the discrete measure of entropy defined by

$$H = -\sum_{i=1}^{M} \sigma_i' * log\ \sigma_i' \tag{4.7}$$

where the σ_i' are the normalized singular values, i.e. $\sigma_i' = \frac{\sigma_i}{\sum_{i=1}^{M} \sigma_i}$.

We can note that the entropy reflects the number of states of the system: when the complexity increases, the dimension of the manifold will rise and then the number of singular values above the noise floor will increase too. With the definition used, the entropy will rise too. The counterpart is that the entropy is subject to the level of noise. If it rises, then the value of entropy will rise too. In the case of a system with a constant level of noise, the entropy is a good measure to observe the evolution of the system. In the case of EEG data, it is highly improbable that the level of noise (artifacts, overall mental activity, ...) remains constant for several hours. Nevertheless, we will apply this measure to our data and try to deal with the presence of this noise.

4.3.2 Results

To apply the entropy measure to our data, we compute the singular values using the procedure described at the beginning of this chapter. We then compute the entropy for

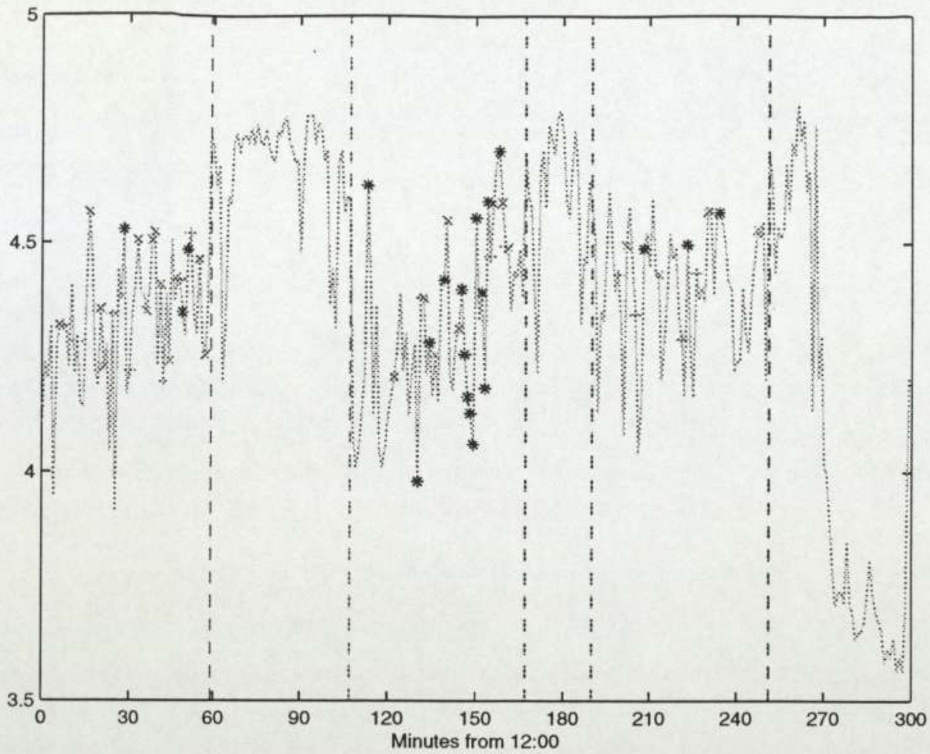

Figure 4.3: **Result of the entropy measure on channel O1:** the stars denote the minutes characterised by a high level of inattention, the dashed lines represent the start and end times of the trials.

each of the 300 sections of one minute. The results computed using data from channel O1 are shown in figure 4.3. Once again, the dashed lines represent the start and end times of breaks/trails and the plus signs, the crosses and the stars represent the events described in appendix A.

Using the figure, we can observe the following points:

- The entropy measure distinguishes the periods of attentiveness from the lunch break and the refreshment breaks. During the break periods, only a few points present lower values of entropy. Among them are all the points after 16:30. These strange values are present in all the defined measures, and are probably due to a recording problem at the end of the day. We have no explanation for these points due to the absence of video record or any information. In the same way, at the beginning and at the end of each break, we can observe peaks with low values of entropy. These periods occur during the EOG test, and can be explained by the behaviour of the observer: the tests require attention and during several minutes the subject is as attentive as during the experiments. It seems then normal to observe the same measure as during periods of concentration (this remark is true for the previous measures).

- The analysis of the video tape tells us that the fourth trial is characterised by a large number of small movements from the subject. On the plot we can see that the curve presents on average higher values than during the two other trials. the reason of this effect could be either a bigger complexity of EEG or a higher noise. At present we have no way to choose between these hypotheses.

- Finally, the entropy measure does not allow us to isolate the sections which are considered as sections of inattention (except the separation between trials and breaks).

4.3.3 Improvements

The entropy function considers all singular values, including a large part of noise dominated eigenvalues. Could it be possible to modify the entropy measure to consider mainly the singular values which are not dominated by the noise ?

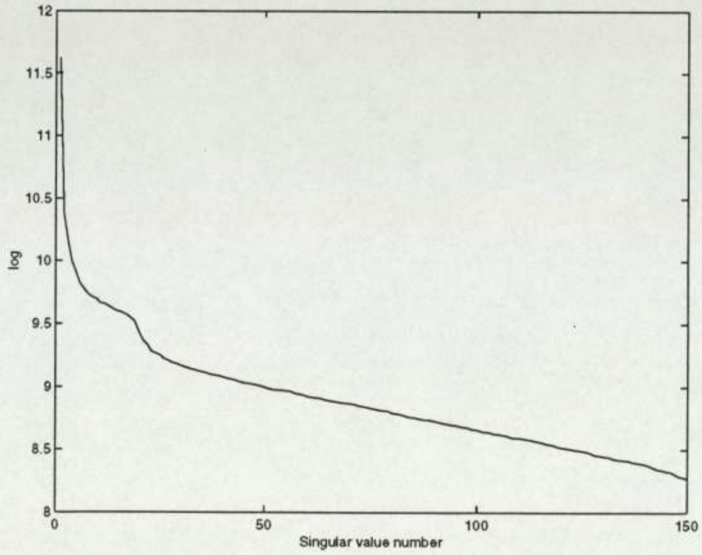

Figure 4.4: **Spectrum of singular values of channel O1**

Consider the embedding matrix composed of 5000 embedding vectors chosen at different times of the day (with a window size equal to 150). This matrix represents then the mean state of the channel during the day. Using the singular value decomposition, the scree test on the spectrum of singular values allows us to compute the complexity of this matrix (figure 4.4). Here, the scree test supposes an average complexity of about 20.

This values suggests that only the 20 first eigenvalues are not noise dominated. A variant of the proposed entropy measure could then be to only consider the 20 first eigenvalues in the computation of the entropy. The new entropy measure is shown in figure 4.5. The main observation is the presence of a floor for entropy during the experiments. the variations between points during trials are reduced. The main peaks above this floor correspond now to periods where the subject was eyes closed or half closed (minutes 145 to 151 and 152 to 154) or when she was eating and talking with an experimenter for half a minute (minute 113). Nevertheless one half of the test points (the stars) stay in the floor, which does not allow us to use entropy to realise a classification.

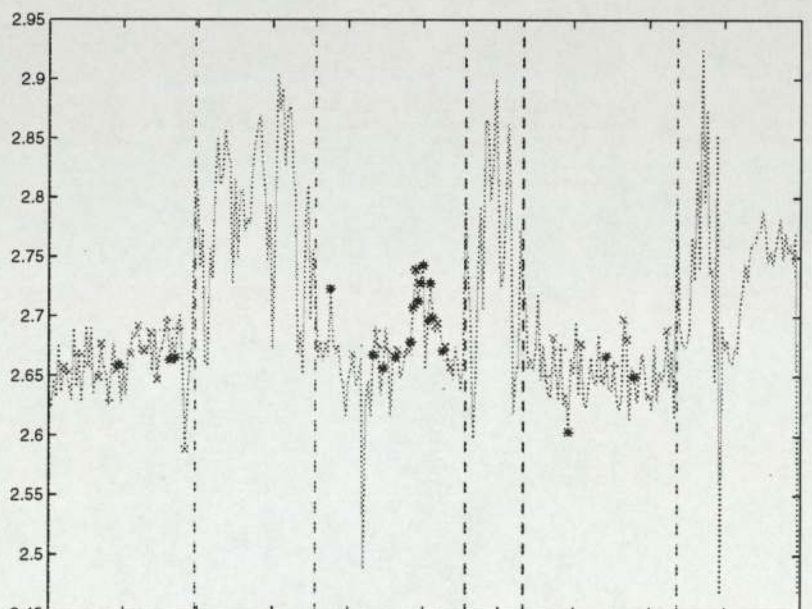

Figure 4.5: **Entropy measure restricted to the 20 first eigenvalues of channel O1**

Previous results suggest us that the channel O1 is not the best channel to identify the periods of inattention (Cf. the remark page 35). The results using channel O2 and P4 are presented in appendix B.3.

The differences between the results of the two entropy measures suggest that the shape of the spectra could inform us about the activity and about the concentration of the subject. We will now inspect a measure which will emphasise the 'shape' of the values and not the values themselves.

4.4 Fisher's Information based measure

4.4.1 Definition

In statistical sciences, a more common measure of information content is Fisher's Information. It was proposed by Fisher in 1934. The Fisher's Information $I_n(\theta)$ is defined as the "amount of information" (information about θ) in a sample of n independent observations. Its definition is [16]

$$I_n(\theta) \;=\; E\left[\left(\frac{\partial ln\ L}{\partial\theta}\right)^2\right] \tag{4.8}$$

where L is the likelihood of the sample.

Fisher's Information can also be defined for a function G by [16]

$$I(x) \;=\; E\left[\left(\frac{\partial ln\ G}{\partial x}\right)^2\right] \;=\; E\left[\frac{1}{G^2}\left(\frac{\partial G}{\partial x}\right)^2\right] \tag{4.9}$$

To compute our measure, we apply this formula to the discrete function G defined by $G(n) = \sigma'_n = \frac{\sigma_n}{\sum_{i=1}^{M}\sigma_i}$, using for the first derivative $\frac{\partial G}{\partial x} = \sigma'_i - \sigma'_{i+1}$. The formula we use for the measure is then

$$I \;=\; \frac{1}{M-1}\sum_{i=1}^{M-1}\frac{(\sigma'_i - \sigma'_{i+1})^2}{(\sigma'_i)^2}, \qquad \text{where } \sigma'_i = \frac{\sigma_i}{\sum_{i=1}^{M}\sigma_i} \tag{4.10}$$

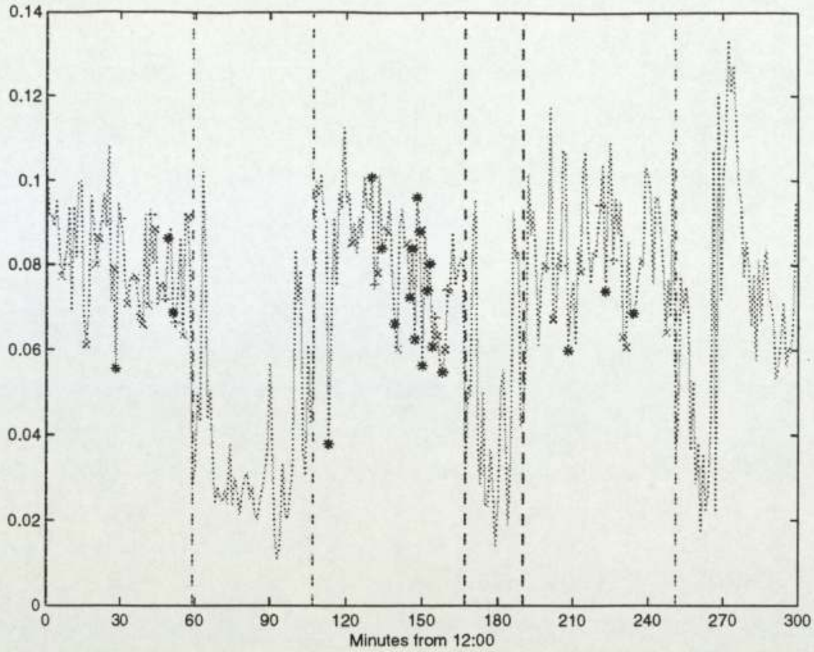

Figure 4.6: **Fisher's information based measure applied on channel O1**

4.4.2 Results

To apply the measure, we use the same procedure as for the entropy, i.e. we compute the singular value decomposition for each minute from 12:00 and 17:00 and we calculate the measure on the resulting singular values. The resulting graph is shown in figure 4.6.

Once again, the measure separates the periods of experiments from the other periods of the day but the Fisher's Information based measure highlights a larger number of periods of attentiveness than the first entropy measure. But the measure is still unable to select all these points, so we may expect an improvement using the same criterion as we used for entropy.

When we compute the Fisher's measure restricted to the 20 first eigenvalues, we do not observe major differences between the two graphs. This may suggest that the major part of the Fisher's information is contained in the first eigenvalues. Actually, the first 5 eigenvalues represent more than 95 percent of the total of the Fisher's information. During the visual inspection, we observed different kinks of curve, but due to the predominance of the first singular values, the measure does not reflect the

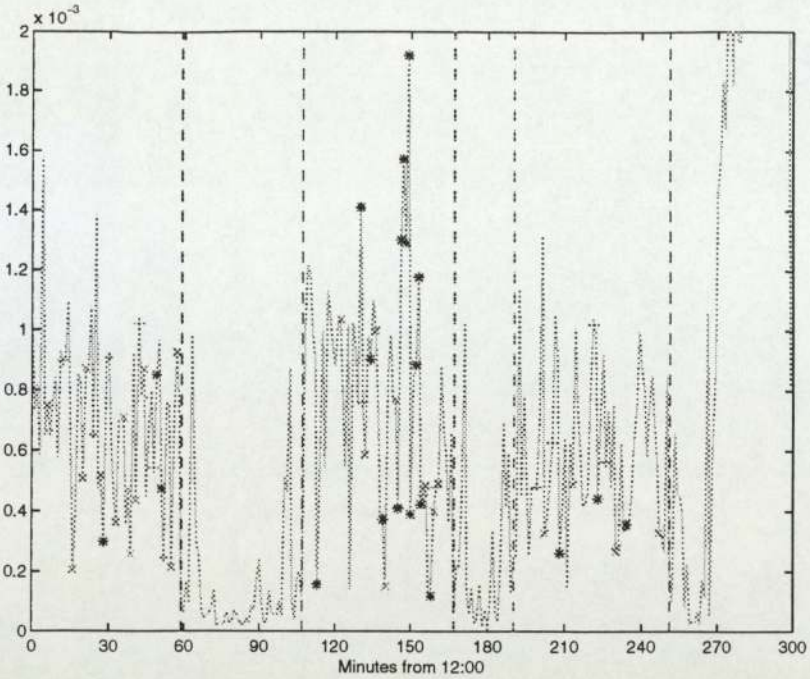

Figure 4.7: Fisher's information based measure restricted to singular values between 5 and 150

variation of the shape.

The improvement we propose is to remove these first terms in the computation of the measure, and just to consider the eigenvalues from root number 5 to 150.

The modified measure will then be:

$$\text{Restricted Measure} = \frac{1}{M-6}\sum_{i=5}^{M-1}\frac{(\sigma_i' - \sigma_{i+1}')^2}{\sigma_i'}, \qquad \sigma_i' = \frac{\sigma_i}{\sum_{i=1}^{M}\sigma_i} \tag{4.11}$$

The graph obtained with this measure is shown in figure 4.7. We observe that the periods of rest (lunch break for instance) are characterised by lower values of the measure. It is true too for some times during the experiments when the subject is moving (minutes 28 and 158 when she stretches and minute 113 when she eats and talks with the experimenter) and for some events characterised by movements (represented by crosses). Alternatively, the periods when the subject dozes off are characterised by higher values (around minute 150).

4.5 Angular Measure

Finally, a last measure is presented. This measure is not related to the complexity contrary to the other measures of this chapter. Previous work considered only the eigenvalues of the covariance matrix. In this section we will use the other parameters obtained when computing a PCA or a singular value decomposition.

Considering the flow of embedding vectors, the singular values represent the parameters of cloud formed by these vectors in the embedding space. The variation of the eigenvalues will then characterise the variations in size of the cloud. The second kind of parameters which is available with a PCA is the main directions of the cloud. These directions are given by the eigenvectors computed during the PCA.

Considering two successive decompositions, we may order the eigenvectors by their eigenvalues, from the biggest one to the smallest one. We can then compare the eigenvectors of corresponding rank. Here, we will compute the cosine of the angle formed by these successive vectors using the definition of the scalar product:

$$\cos\ \theta_i(t) = \frac{v_i(t) \cdot v_i(t+1)}{||v_i(t)|| * ||v_i(t+1)||} \tag{4.12}$$

This angular measure is then computed for the 300 minutes between midday and 5 o'clock for the 150 different eigenvectors. Of course, only the measures corresponding to about the 10 first directions have meaning: when the order increases, the eigenvectors become more and more subject to fluctuations due to increases of noise level.

The following figure presents the angular measures computed for the 5 first series of eigenvectors. The changes in the directions of the cloud appear mainly during periods of doze or weariness (around minutes 150 for example) when there is fewer movements but during the periods of rest, the angular measure stays constant.

4.6 Discussion

The first aim of this project is to try to characterise vigilance using EEG. In this chapter we investigate several measures of complexity, expecting a correlation between

Figure 4.8: **Angular measure applied to channel O1:** the measures are applied to the 6 first series of eigenvectors, from the most significant (top) to the less (bottom on next page).

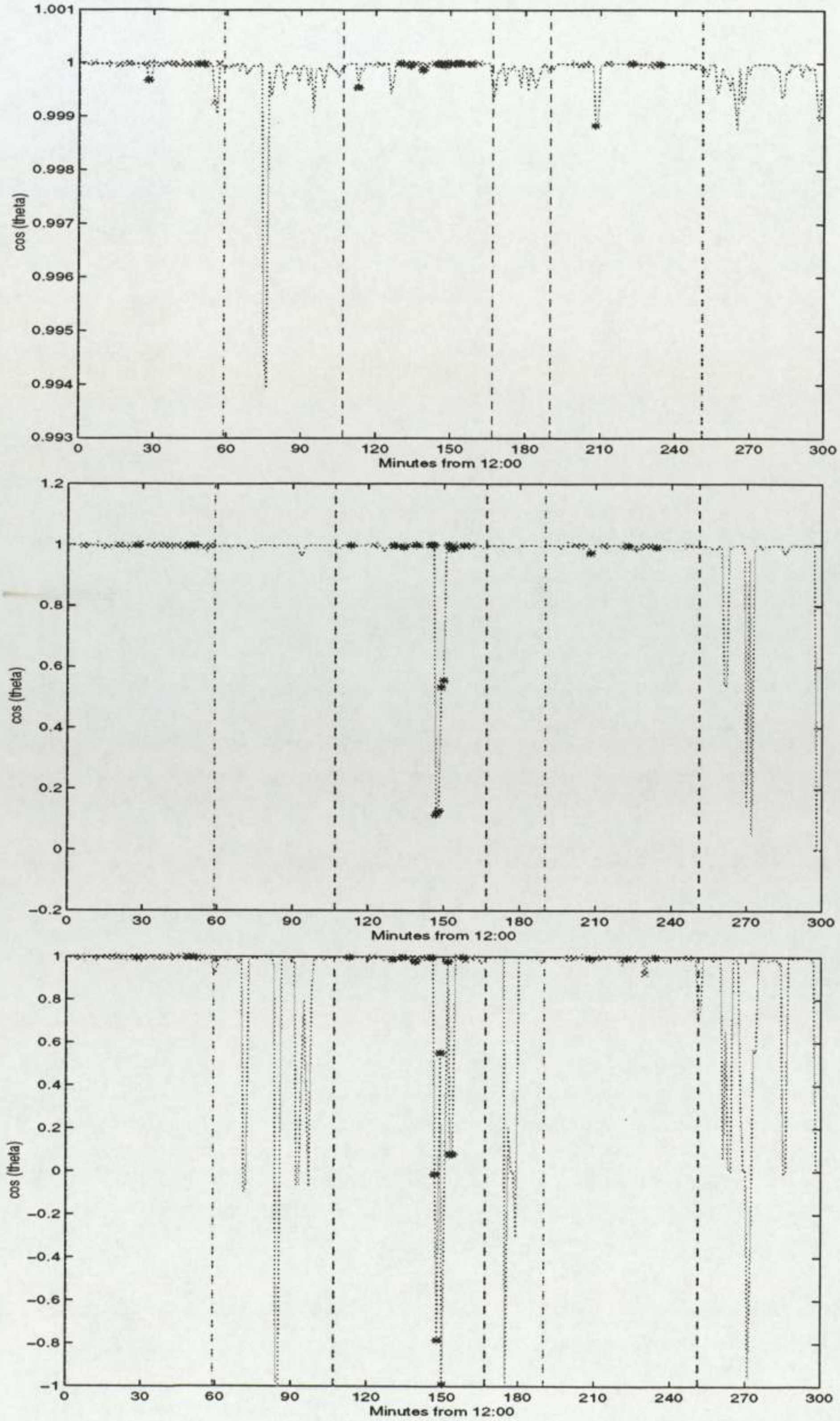

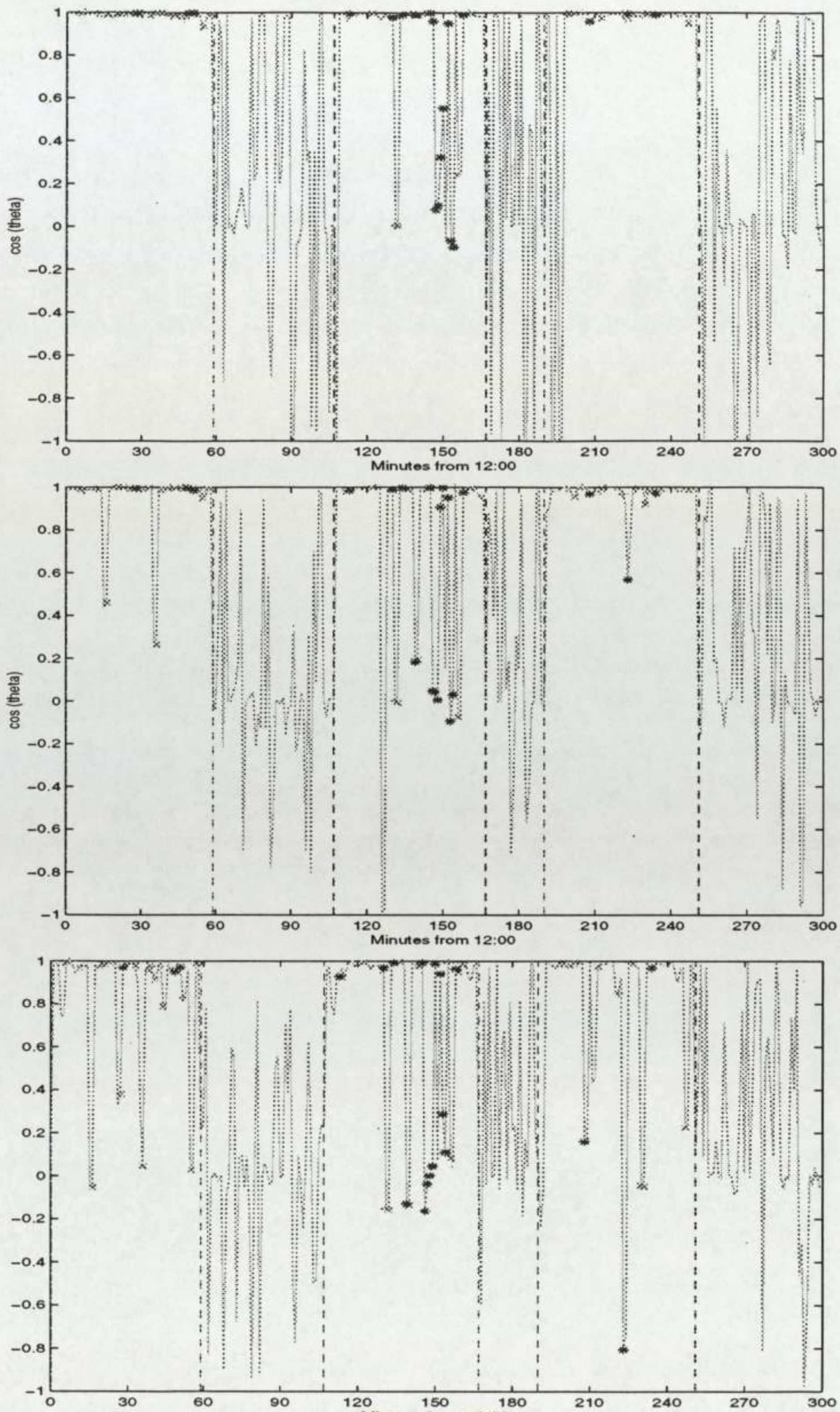
cos (theta)
Minutes from 12:00
cos (theta)
Minutes from 12:00
Minutes from 12:00
1
0.8
0.6
0.4
0.2
0
−0.2
−0.4
−0.6
−0.8
−1
0 30 60 90 120 150 180 210 240 270 300

the behaviour of the subject and the complexity of EEG.

The simplest measure we presented, the scree test, is a very subjective method, which requires the visual inspection of a large number of spectra. This first measure provides some interesting results. First, just using the value of this measure, we can cluster the rest periods from experiments. One explanation could be the presence of artifacts due to the movements during the lunch or the refreshment breaks. But if we consider the beginning and the end of each tasks, we can observe that peaks in the curve of the number of significant singular values. These peaks correspond to the calibration tests: for one or two minutes, the subject is waiting for the experimenters and for the tests. During these periods, she remains sitting and she do not move and we observe a low value like during the lunch. So this measure does not only measure the presence of artifacts. This remark is still valid for the other measures.

To remove the subjective analysis, we then defined four simple measures, but they are not completely objective due to the presence of an arbitrary threshold in their definition. Nevertheless, these five measures show us that the singular spectra contain enough information to distinguish the periods of activity from the break periods. More, these four measures are able to reproduce the results of the visual inspection with less subjectivity. But the problem is that we have no criterion to determine if a measure is a good measure. We then use information obtained using the video tape to compare the different measures, expecting to a good measure to be able to cluster the break periods and the sections of inattention (represented by stars on the plots).

As a complete objective measure, we then use the entropy measure. This measure and its improvement allow us to detect few periods of inattention during the afternoon, but not all of them. To improve this detection and to emphasise the 'shape' of the spectra, a measure based on the slope of the spectra is proposed. This measure presents better results in term of separation of the periods of inattention during the trials. It may suggest that the shape of the singular spectra vary with the attention of the subject.

Finally, a last measure is presented. Contrary to the other measures, it is not related to the complexity but it measures the variation of the main directions of the manifold. It tells us that the principal directions of the manifold are relatively constant except for few times, principally during the breaks and during the mini-sleep periods. The results of this measure differ from the results of the previous measures. The angular measure presents the best results in term of separation between the periods of inattention during the tasks and the rest of the experiments. Another point is that it remains constant during the break periods. Future work could then be to study more closely this measure to understand the reasons of the variations of the angular measure. This measures is also probably the best measure to classify the periods with events of groups 3 and 4 (described in appendix).

Chapter 5

Feature Extraction

5.1 Independent Component Analysis

Recently, Independent Component Analysis has been used in several studies to remove the artifacts from multi-channel EEG with promising results [7], [6] as well from single channel EEG [8]. In this section, we choose to perform an ICA decomposition on our data and then to apply the previous measures on the results of this decomposition.

The goal of ICA is to recover independent sources given only records that are unknown mixtures of these sources. In contrast to correlation-based transformations such as Principal Component Analysis, ICA not only decorrelates the signal (using 2^{nd} order statistics) but also reduces higher-order statistical dependencies, attempting to make the signals of the decomposition as independent as possible. In other words, Independent Component Analysis attempts to produce projections by finding directions (not necessarily orthogonal, contrary to PCA) which are statistically independent.

Several methods have been proposed for Independent Component Analysis. Here, we will use the algorithm proposed by Hyvärinen and Oja [5], the fast-fixed point algorithm.

5.2 Independent Component Analysis on the EEG data

The aim of the feature extraction is to improve the signal by selecting some of its characteristics. Here, we expect to be able to separate the noise (i.e. the sources containing a lot of signals with frequencies beyond 50 Hz) from the normal waves of the brain (alpha and beta activities). We can then improve the signal by removing the noise components. We wish afterwards to apply the previous measures to the result of the extraction.

To extract the different sources of the signal, we perform ICA on an embedding matrix which represents the period 12:00–17:00. We choose this approach instead of dividing the data in epochs because we wish to apply the same linear transformation to all our data. If we do not always use the same projection, we may modify the dynamics of the time series by introducing differences between the different periods of the day.

To construct the embedding matrix, we construct the delay vectors from the time series with no overlapping, using a window size of 150. The size of this trajectory matrix is then 150 rows for about 30000 columns.

Because we do not know how many sources are present in the signal, we compute as many independent components as we have delay vectors i.e. 150 independent components. We then select the sources according to their power spectra. The following figures present some interesting sources. The plots of sources are reduced to a length of 10 seconds for more clarity. They correspond to the 10 first seconds after midday.

Among the 150 sources, a large number of them have their power spectra characterised by the presence of high frequencies, such as the 97^{th} source (5.1 (h)), so we exclude them from the rest of the computation. The study of the power spectra shows us that only 22 sources are not dominated by noise, i.e. they have the major part of their frequencies below 50 Hz. In figure 5.1 (b) to (g), some of these sources are presented.

- the 52^{th} source (*b*) corresponds to frequencies below 3 Hz. It may suggest that this

Figure 5.1: **Independent sources and their power spectral densities**

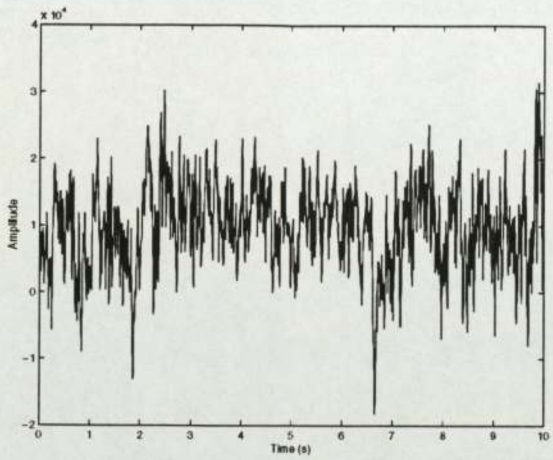

(a) *Original signal*

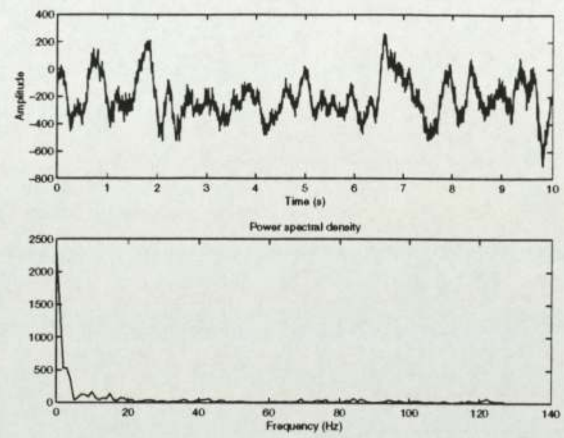

(b) 52^{nd} *source*

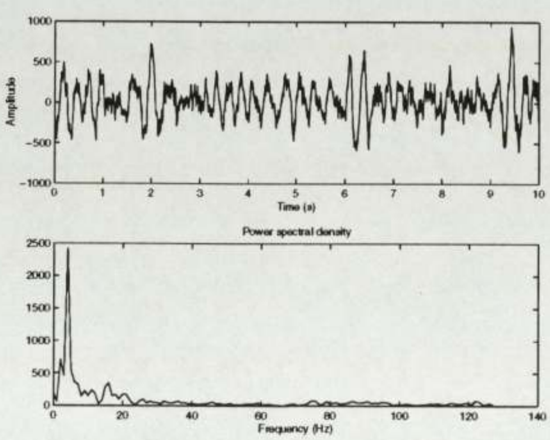

(c) 150^{th} *source*

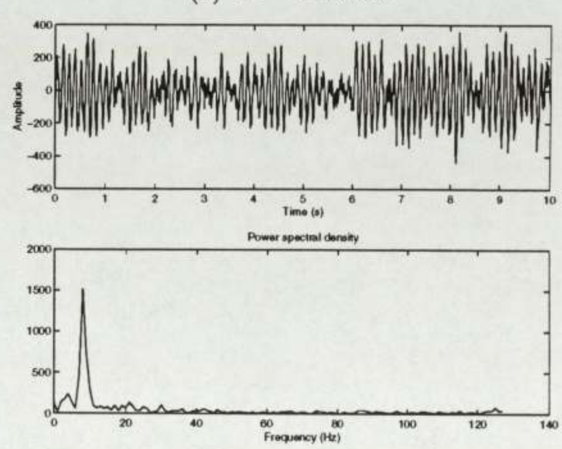

(d) 106^{th} *source*

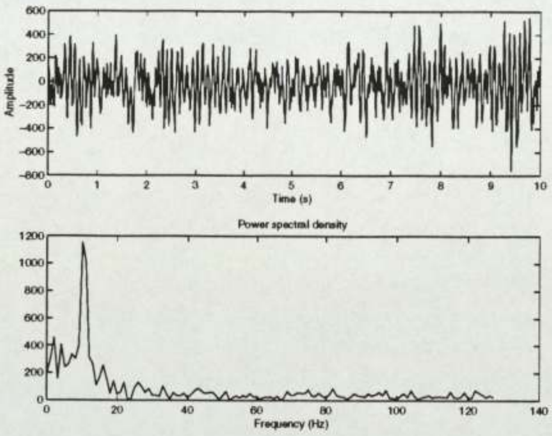

(e) 145^{th} *source*

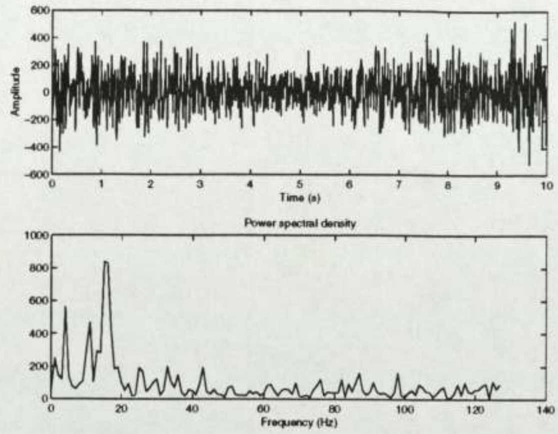

(f) 139^{th} *source*

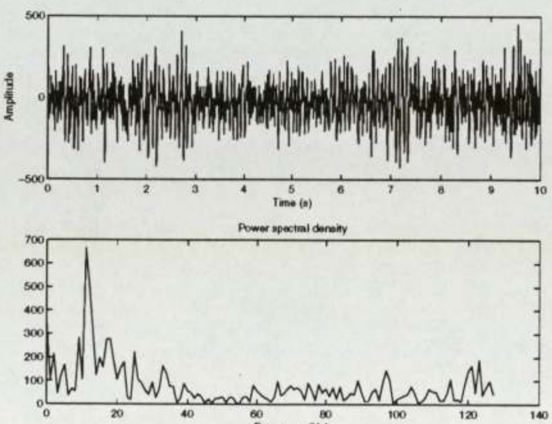

(g) 137^{th} *source*

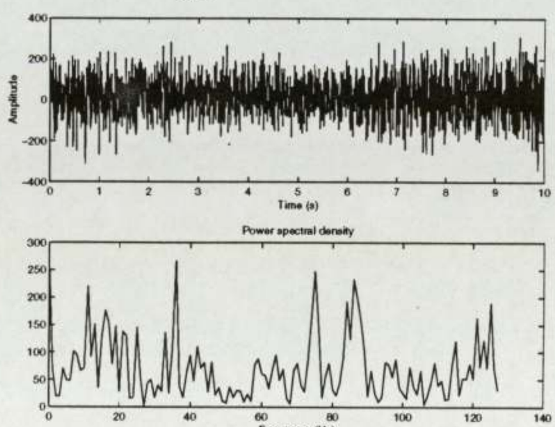

(h) 97^{th} *source*

source corresponds to a muscular activity (eyes movements or hands movements). In terms of frequency bands, this range corresponds to the delta activity.

- the 150^{th} source (c) corresponds to frequencies in the theta bands.
- sources 106 and 147, (d) and (e) have frequencies characterising the alpha activity.
- source 139 shows us some beta activity, with a peak in the power spectrum near 18 Hz.
- source 137 shows us a mixture of alpha and beta activity.

It is difficult to give a good interpretation of these sources, particularly for the sources in the theta and delta bands because they correspond to abnormalities if they are present in the raw EEG signal.

5.3 Results

The study of the power spectra tells us that only 22 sources are not dominated by noise, with no frequency beyond 50 Hz. More, these sources present always the same power spectra at different times of the day, so it may suggest that the ICA isolate the sources of the dynamics of the EEG.

The first goal of our feature extraction was to try to improve the signal to noise ratio to improve the measures of complexity. By projecting the embedding vectors on the 22 selected independent components, we are able to reduce the proportion of the noise in the signal. We will now try to apply the measures of the complexity to the results of the feature extraction.

In the previous chapter, we applied the measures to the results of the singular values decomposition of the trajectory matrices. Now, the trajectory matrices are projected in a smaller vectorial space, the feature space ($\mathbb{R}^{22}$). The singular value decomposition is then now applied on the projections of the trajectory matrices instead of the matrices themselves. The two measures (entropy and Fisher's Information based measure) are then computed using the resulting singular values spectra.

5.3.1 Results with entropy

The figure 5.2 presents the results of the entropy measure when we use the ICA decomposition of the signal. Now, almost all periods of inattention are clustered by the measure. Only four of them stay in the floor. More, all the points corresponding to mini-sleep periods are now at the same level as the periods of break. Once again, the third trial is characterised by higher values of entropy than the two others.

Contrary to the improvement of entropy measure proposed in section 4.3.3, the entropy measure of this section does not cluster the periods of activity/break as well as the improvement, but it allows to separate more points from the floor.

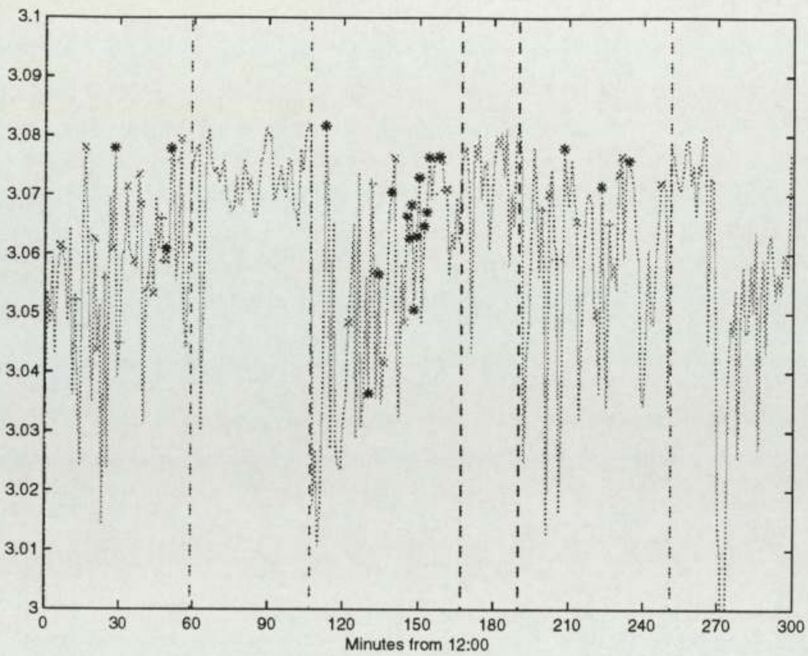

Figure 5.2: **Entropy measure after ICA decomposition**

5.3.2 Results with Fisher

In the same way, the Fisher's Information based measure introduced in section 4.4 was applied on the singular values computed using the projected data. The results are shown in figure 5.3. The first remark is that the Fisher's measure does not cluster as many test points (the stars which represent the periods of inattention) as the entropy measure in the previous figure, but these points are now more distinct from the other points. An interesting effect appears at the end of the first trials (period 12:00–12:59). This effect does not appear with any of the other measures proposed. We have no explanation for it.

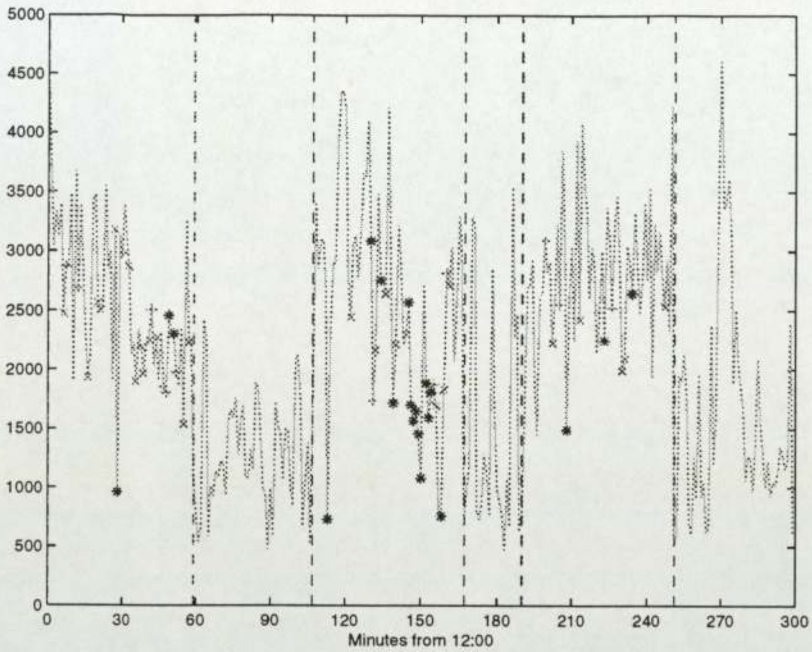

Figure 5.3: **Fisher's Information based measure after ICA decomposition**

5.4 Discussion

In this chapter, we try to perform a feature extraction on our data in order to reduce the noise in the signal. The method we use consists of an ICA decomposition using the algorithm proposed by Hyvärinen and Oja, the fast-fixed point algorithm [5]. ICA decompositions are usually performed on multi-channel records, but according to [8], ICA can cluster the different sources of EEG signals even using a single channel recording.

On our data, ICA decomposition allows us to isolate a large range of noise and remove them from remaining sources. We also recover some sources which seem to correspond to the brain activity such as alpha activity, beta activity, etc.

Using 22 sources which do not have noise in their spectra we then try to characterise the projection of the embedding vectors using the last two measures presented in the previous chapter, i.e. the entropy measure and the measure based on the Fisher's Information.

The results of these measures are interesting. They allows us to discover new effects which are not visible with any other measures, as well they better classify the periods of inattention from the other periods of the trials. The main problem with the comparison of the different measures is that we do not have any criterion to order the results of the measures, and the method we used, the clustering of periods of inattention, is subject to the analysis of the video tape, and these test periods occur only on a few occasions.

Chapter 6

Conclusions

Throughout this thesis, we have used a technique called *embedology*, more precisely a class of embedding method known as *Taken's method of delay* [18], [2] and [17]. The strength of this method is that it allows to study the dynamical properties of the underlying generators of the data by reconstructing an image of the manifold in an embedding space. Even if the attractor is deformed, the topological properties are preserved.

The main problem with embedology is the absence in the theory of criterions to choose correct values for the parameters of the embedding. In this thesis, we proposed a method based on the convergence of the singular spectra. We do not know if this criterion allows us to find correct values for the window size and for the number of delay vectors, but it allows us to reduce the effects of these parameters on the spectra of singular values. It is then a good criterion in our case because the presented measures depend in the majority on the singular values. Another interesting point is that annex B.1 shows that the results are consistent across different electrodes.

Using the embedding approach and the singular value decomposition, we then propose several measures of complexity. The first measure we proposed, the scree test attempts to determine the number of significant singular values. This method is rather subjective, so we then proposed alternatives to the scree test. These alternative are able to reproduce the results of the scree test but are still dependent on subjective parameters due to the presence of a threshold in their definitions. As a completely objective measure, we then computed the entropy measure and a measure based on the Fisher's Information measure used in statistical sciences.

The results of all these measures are quite promising: they all allow us to isolate the trials from the breaks and they can detect some periods of inattention but not all the periods. The definite distinction between the periods of activity and the break periods can however be interpreted as an effect of the level of artifacts due to the movements of the subject. In the same way, all the measures clearly distinguish the minute 113, when the subject eats her apple and talks to the experimenters for half a minute. Nevertheless, some measures isolate the periods around minute 150 (14:30) from the other points. During this period, the observer is subject to mini-sleep periods, characterised by few movements, eyes closed, etc. So we can expect that if the presented measures are sensitive to the muscular activity, they record too some information about the brain states.

The main difficulty we encountered is that we have no criterion to compare the different measures we proposed: as mentioned in the second chapter, the performance measure recorded by the task program is very weakly correlated with the behaviour of the subject observed using the video tape. We then used the observations obtained using the video tape to compare the measures, which is probably not the best way to compare them. A possible future work could be to develop a scoring method of these measures, for instance by computing the percentage of (mis)classified sections. No measure is able to correctly classify all the sections of inattention so the suggestion for a future work could then be to try to use the results of the different measures as input of a classifier.

In a third part, to improve the signal to noise ratio, we apply an ICA decomposition to our data. On the results of this decomposition, we then compute the entropy measure and the Fisher's Information based measure. These two measures give better results in terms of separation between the periods of inattention and the rest of the trial periods.

Finally, in this thesis, we computed the measures for several channels and we compare the results, but we use EEG data recorded only on one subject, so we do not know if the results we observed are particular to one subject or if they can be extended to other people.

Bibliography

[1] CM Bishop. *Neural Network and Pattern Analysis.* Oxford University Press, 1995.

[2] DS Broomhead and GP King. Extracting Qualitative Dynamics from Experimental Data. *Physica D*, 20:217–236, 1986.

[3] R Cattell. The scree test for the number of factors. *J. Multiv. Behav*, 1:245–276, 1966.

[4] A Hyvärinen. Survey on Independent Component Analysis. *Available from http://www.cis.hut.fi/~aapo/.*

[5] A Hyvärinen and A Oja. A fast-fixed point algorithm for independent component analysis. *Neural Computation*, 9:1483–1492, 1997.

[6] TP Jung, C Humphries, TW Lee, S Makeig, M McKeown, V Iragui, and TJ Sejnowski. Extended ICA Removes Artifacts from Electroencephalographic Recording. *Advances in Neural Information Processing Systems*, 10:894–900, 1998.

[7] TP Jung, C Humphries, TW Lee, S Makeig, MJ McKeown, V Iragui, and TJ Sejnowski. Removing Electroencephalographic Artifacts : Comparison between ICA and PCA. *Neural Networks for Signal Processing VIII, Proceeding of the 1998 IEEE Workshop*, pages 63–72, 1998.

[8] D Lowe. Feature Space Embeddings for Extracting Structure from Single Channel Wake EEG using RBF Network. *Neural Networks for Signal Processing VIII, Proceeding of the 1998 IEEE Workshop*, 1998.

[9] D Lowe and N Hazarika. Complexity modelling and stability characterisation for long term iterated time series prediction. *Applications and Science of Artificial Neural Network*, 440:53–58, 7-9 July 1997.

[10] S Makeig, A Bell, T jung, and T Sejnowski. Independant Component Analysis of Electroencephalographic Data. *Advances in neural Information Processing Systems*, 8:145–151, 1996.

[11] S Makeig and M Inlow. Lapses in alertness: coherence of fluctuations in performance and eeg spectrum. *Electroencephalography and Clinical Neurophysiology*, 86:23–35, 1993.

[12] S Makeig and TP Jung. Changes in alertness are a principal component of variance in the EEG spectrum. *NeuroReport*, 7:213–216, 1995.

[13] P Nunez. *Neocortical Dynamics and Human EEG Rythms.* Oxford University Press, 1995.

[14] IA Rezek and SJ Roberts. Stochastic Complexity Measures for Physiological Signal Analysis. *IEEE Transactions on Biological Engineering*, 44(9), September 1998. *Available from http://www.ee.ic.ac.uk/research/neural/irezek/publication.*

[15] IA Rezek and SJ Roberts. Temporal and Spatial Complexity Measures for EEG-based Brain-Computer Interfacing. *Medical and Biological Engineering and Computing*, March 1998.
Available from http://www.ee.ic.ac.uk/hp/staff/sjrob/Pubs.

[16] G Saporta. *Probabilités, analyse des données et statistique.* Edition Technip, 1990.

[17] T Sauer, J Yorke, and M Casdagli. Embedology. *Journal of Statistical Physics*, 65:579–616, 1991.

[18] F Takens. Detecting strange attractors in turbulence. *Lecture Notes in Mathematics*, 898:366–381, 1981.

Appendix A

Analysis of the video tape

This appendix presents the abnormal behaviours of the subject during the three trials. In the following table we have reported all events which seem to be interesting for the study, for example abnormal behaviours (eating, drinking), movement (for the presence of artifacts in the EEG), moments of inattention (periods with eyes fully or half-closed, periods when the subject is not looking at the screen, ...) or clues for tiredness (yawn, ...).

The events have been ordered in four groups. The two first groups just denotes clues or behaviour which may reveal loss of attention contrary to the two last groups which indicate that the subject is inattentive to the experiment, for instance not looking at indications on the screen or sleeping.

- The first group consists of events which can produce artifacts in the EEG signals and are not related to attentiveness, but nevertheless, present in a large proportion, they can be clues for tiredness. They are mainly movements of the left arm, to scratch the head, to rub the eyes or the face near the sensors, and so on. They are just reported to detect abnormalities in EEG, for example in case of loss of contact when scratching the head.
- The second group corresponds to the events which can raise the number of artifacts (by increasing the muscular activity) and which can be used as clues for attentiveness. These events can be interpreting as attempts to recover attentive-

ness: changes of position, movements in seat to find a better position, etc. Yawns are also reported in this group.

- The third group is the set of events incompatible with the experiments. On these periods, we are sure that the subject is not attentive to events on the screen, for example because she is eating, drinking, speaking with the experimenters, not looking at the screen, stretching or because she is not holding the joystick.
- The last group denotes periods of complete loss of attention, for example periods of drowsiness with eyes closed or half-closed.

A.1 Trial 2: 12:00-12:59

Table A.1: Events during trial 2

Level	Time	Event	Duration
	11:59:30	**Beginning of trial 2**	
2	12:06:55	Movements, looking for a new position	10 s
1	12:07:42	Movements of left arm	40 s
1	12:12:40	Movements of left arm	25 s
2	12:16:10	Movements, she adopts a new posture	20 s
2	12:20:26	Movements in seat	10 s
2	12:21:03	Yawn	
1	12:24:50	She approaches the screen, she rubs her eyes	
2	12:27:03	She adopts a new posture and yawns	
3	12:28:40	She stretches, scratches her head	
2	12:28:57	She yawns	
1	12:30:35	She rubs her face	15 s
2	12:33:24	Movements	
2	12:36:59	She adopts a new position	
...	...	...	...

Level	Time	Event	Duration
2	12:38:02	New position	
2	12:39:21	New position (closer to the screen)	
1	12:41:41	She scratches her head	10 s
2	12:41:55	Movements	
1	12:42:53	She rubs her face	5 s
2	12:44:05	Movements	10 s
1	12:47:55	She scratches her head	15 s
1	12:48:30	She rubs her left eye	5 s
3	12:49:21	She looks at the ground	5 s
3	12:51:20	She drinks water	15 s
1	12:52:36	She scratches her head	10 s
2	12:55:25	She adopts a new posture	
2	12:55:53	She yawns	
2	12:57:14	Movements	20 s
	12:59:25	**End of trial 2**	

A.2 Trial 3: 13:47-14:47

This trial can be split in two parts. Until the middle of the experiment, the subject seems really attentive to the tracking test except when she eats at minute 113. The second part contrary to the first one corresponds to a period of huge inattention. The maximum of inattention is reached around 14h30, when she has her eyes completely closed for several minutes. This trial can then be considered as a good test for a measure of attentiveness, due to the presence of the complete range of level of attention.

Table A.3: Events during trial 3

Level	Time	Event	Duration
	13:47:36	**Beginning of trial 3**	
3	13:53:18	Eat an apple, Intervention of experimenter	20 s
2	13:56:10	Movements, she adopts a new position	15 s
2	14:02:20	Movements	10 s
3	14:10:27	Stops looking the computer screen	5 s
1	14:11:03	She rubs her eyes	15 s
2	14:12:26	Sigh followed by movements	
3	14:14:35	Loss of attention for 25 seconds	
2	14:16:08	Change of position	
1	14:19:02	Movements of left arm	35 s
3	14:19:40	She scratches her head with her right hand	10 s
4	14:19:50	Eyes closed	5 s
2	14:20:09	New position	
1	14:20:12	She scratches her head with left hand	10 s
2	14:20:30	Yawns and movements	30 s
2	14:24:03	Change of posture	
4	14:25:48	Eyes closed	12 s
2	14:26:00	She adopts a new posture	
4	14:26:47	Eyes half-closed and weariness	13 s
4	14:27:00	Eyes fully closed for 1 minute	60 s
4	14:28:00	Eyes closed	20 s
4	14:29:35	Eyes closed	15 s
4	14:30:06	Eyes closed	5 s
2	14:30:40	Movements, she changes her posture	
4	14:32:36	Eyes half-closed	10 s
...	...	...	...

Level	Time	Event	Duration
4	14:33:35	Eyes half-closed	20 s
3	14:34:10	She stops looking at the screen	10 s
2	14:34:40	Movements	10 s
1	14:35:00	She moves her left arm	
2	14:36:35	Change of posture	
3	14:38:54	She stretches and changes her posture	
2	14:39:35	Change of posture	
1	14:40:07	She scratches her head	
2	14:41:45	Yawn	
	14:47:35	**End of trial 3**	

A.3 Trial 4: 15:10-16:11

This trial could be characterised by a large number of small movements during the experiment. In this trial, the subject is very often moving her arm, changing her posture in the seat, and so on. It should considerably increase the noise due to muscular activity and hide the rest of signal.

Table A.5: Events during trial 4

Level	Time	Event	Duration
	15:11:20	**Beginning of trial 4**	
1	15:19:30	Movements and she rubs her face with her left hand	20 s
2	15:22:00	Movements, she bends forwards for 15 seconds	20 s
1	15:25:30	She rubs her eyes	10 s
2	15:28:40	Movements, Change of posture	10 s
3	15:28:50	Looks at something on the ground	5 s
2	15:31:33	Change of posture	
...	...	...	...

Level	Time	Event	Duration
1	15:41:50	Movements of left arm, she rubs her face	10 s
3	15:43:20	Looks at the ground then at the roof	20 s
1	15:43:55	She rubs her face	10 s
1	15:46:25	She rubs her face	10 s
2	15:50:00	Change of posture	
1	15:50:20	She rubs her face	10 s
2	15:50:37	Change of posture	
2	15:51:00	She yawns	
2	15:51:10	Movements, she bends forwards	
3	15:54:30	Weariness: she closes her eyes	
2	16:07:20	Change of posture	
	16:11:24	**End of trial 4**	

Appendix B

Comparisons between channels

B.1 Comparisons in the choice of the parameters of the embeddings

In section 3.2, we have developed criteria for the choice of the parameters of the embeddings. These criteria were applied only to data from channel O1. We want now to extend them to the different EEG channels to know if the chosen parameters can be used safely.

We then apply the criteria to data recorded from the different regions of the head. The results for the different channels are presented in the following figures (from figure B.1 to figure B.3).

The first interesting point is that we observe a strong convergence of the spectra on all different channels. It suggests that all channels have poor signal to noise ratio. The second point is about the plot of the error functions: all error curves share the same shape and reach a minimum for the same value of window size. So we can conclude that a window size equal to 150 is a good choice. Using the same lag for the different channels will allow us to compare the different measures when applied on different channels.

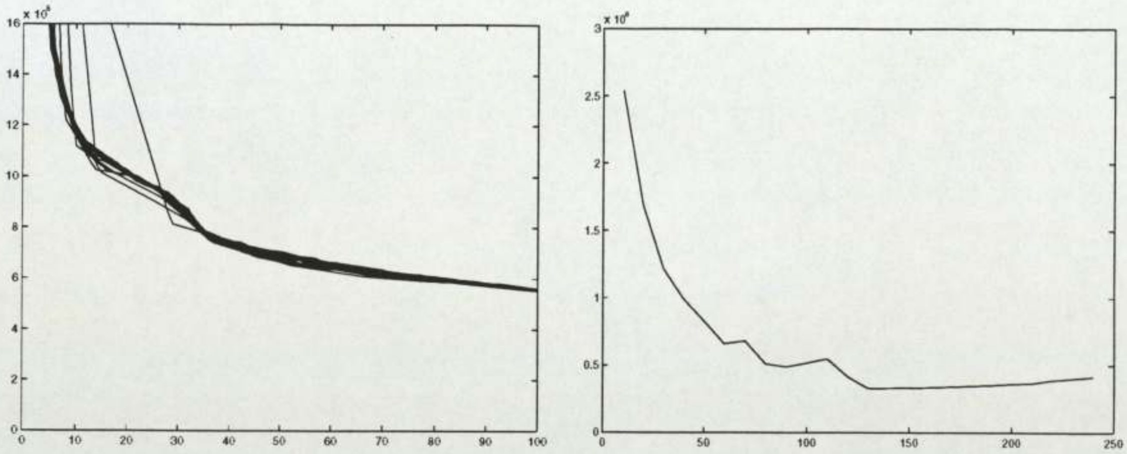

Figure B.1: Convergence of stretched spectra and error for channel O2

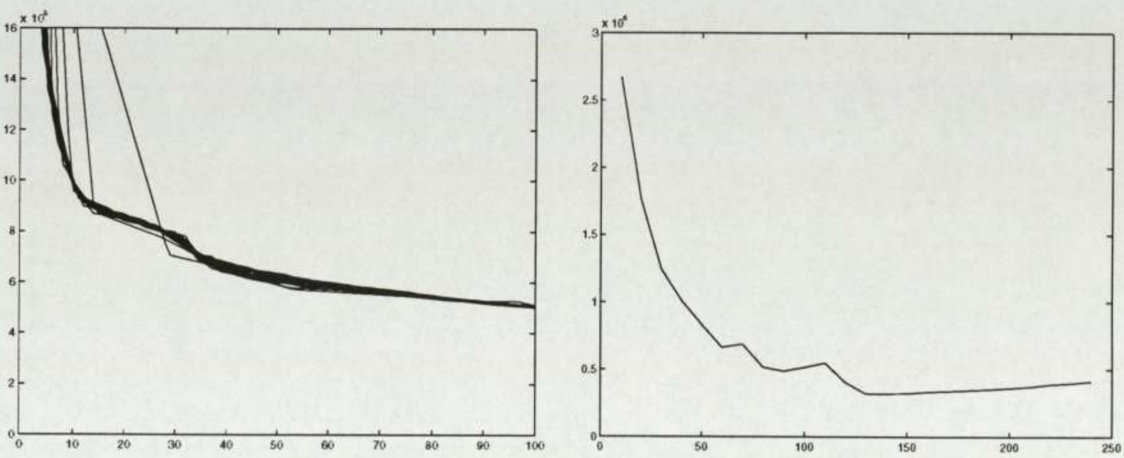

Figure B.2: Convergence of stretched spectra and error for channel P4

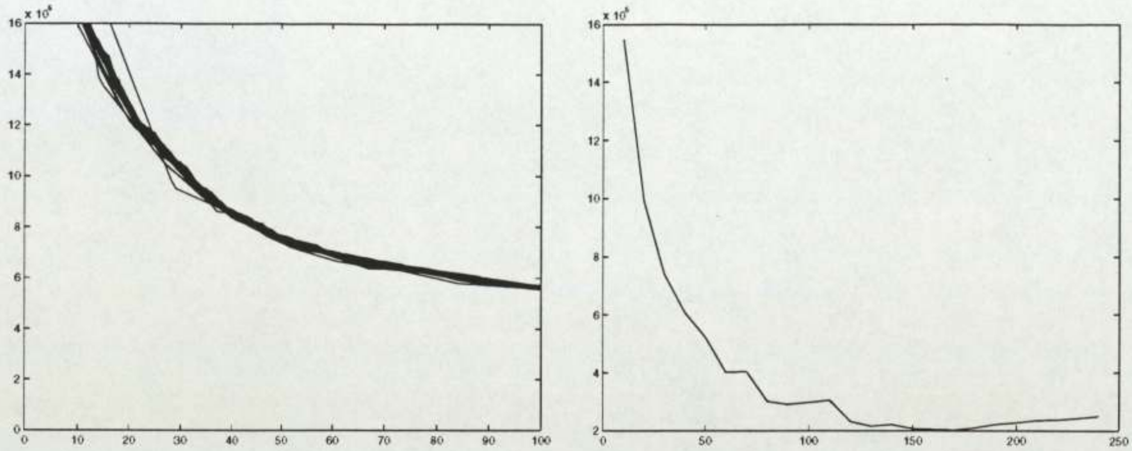

Figure B.3: Convergence of stretched spectra and error for channel FZ

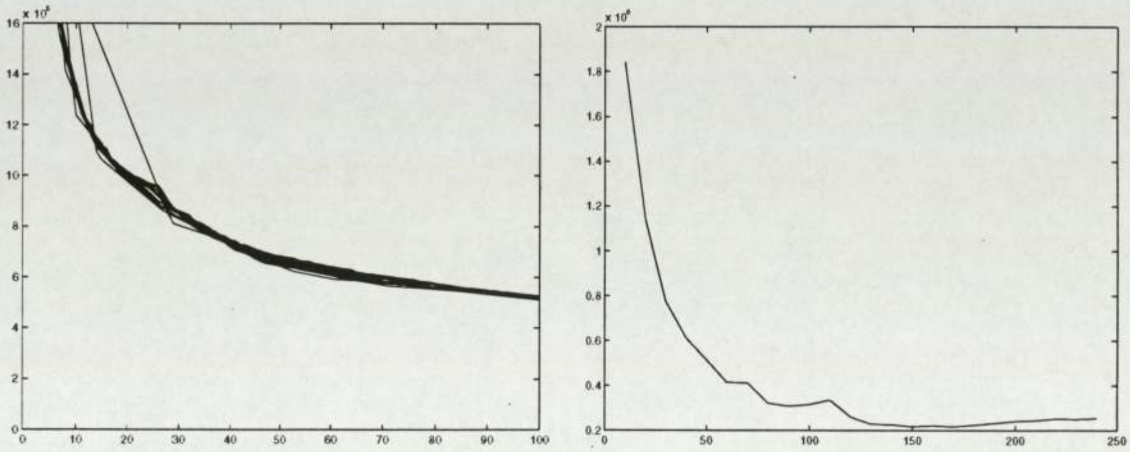

Figure B.4: Convergence of stretched spectra and error for channel C3

B.2 Simple measures of complexity

In this section, we present the results obtained with the four measures defined in section 4.2.3 when applied on channel P4.

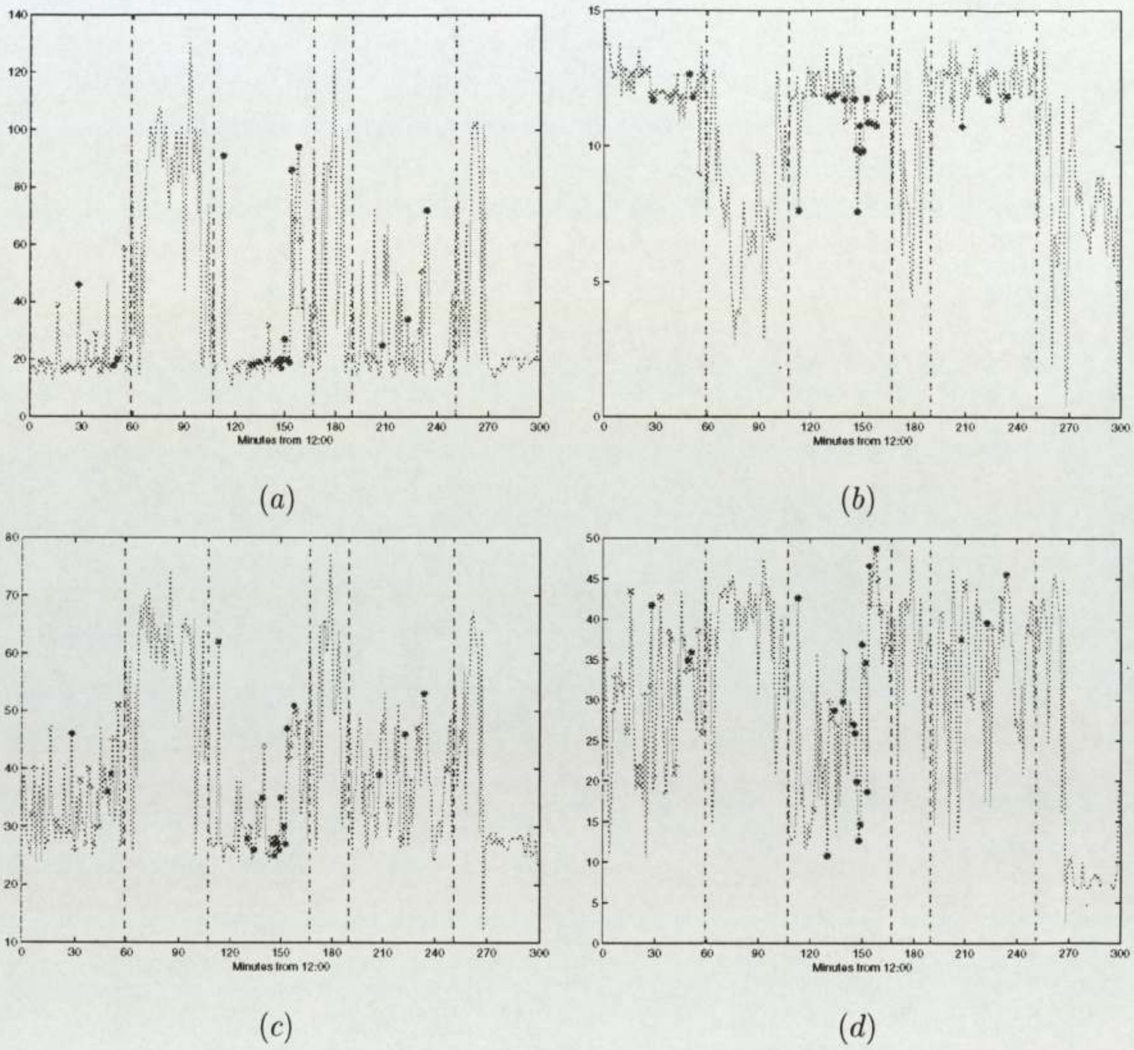

Figure B.5: **Complexity determined using the four measures:** (a) measure M_1 with a threshold of 2500, (b) M_2 with a threshold of 80000, (c) M_3 with a threshold of $7.5 * 10^{-3}$ and (d) M_4 with a threshold equal to 0.5. The stars represent the sections characterized by a poor attention of the subject

B.3 Entropy measure applied to other channels

In section 4.3 about entropy measure, we only applied the measure to channel O1, but previously, on page 35, we said that channels P4 and O1 present better clustering effects for the test points than channel O1. In this section we will apply the entropy measure and its variant on these two channels. The plots of the computation are present on figures B.6 and B.7.

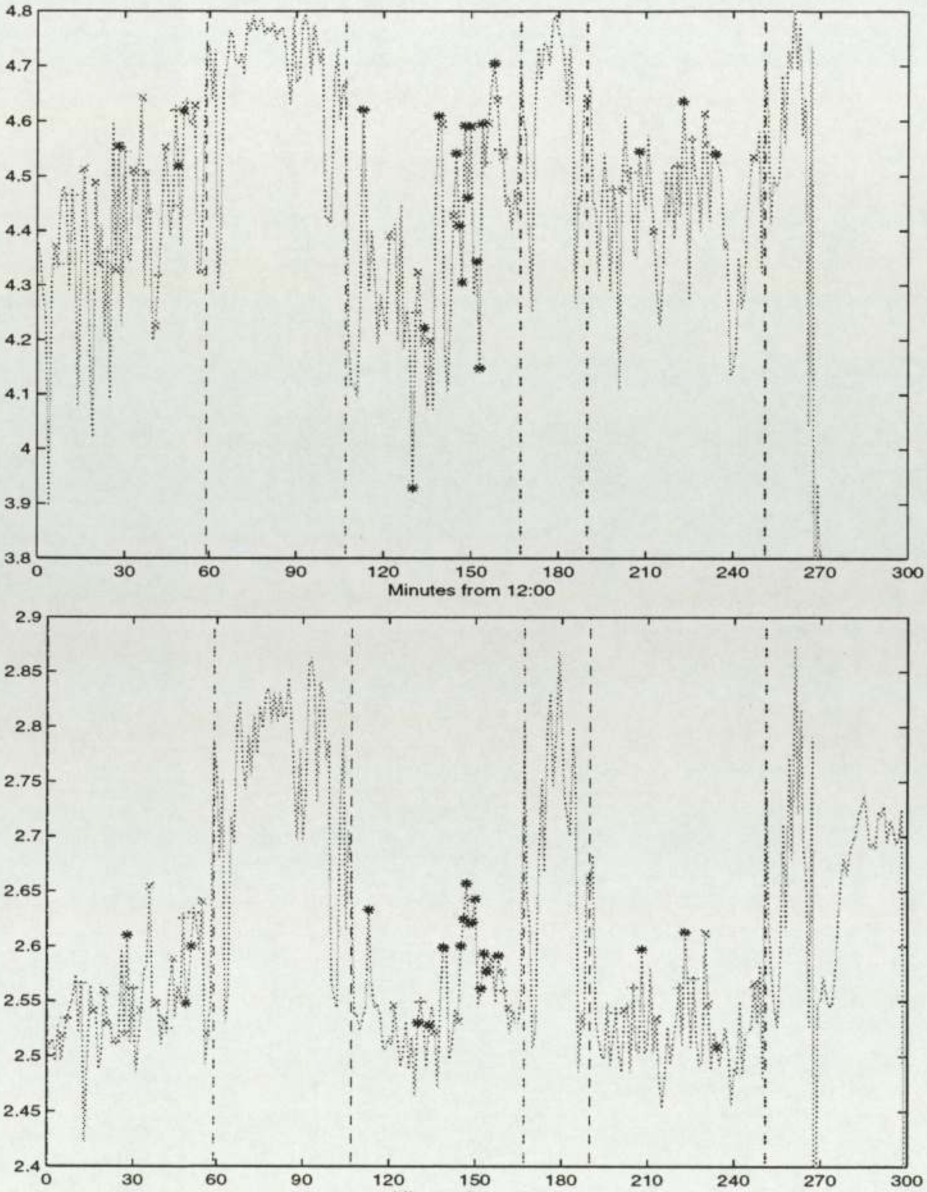

Figure B.6: **Entropy measures for channel O2:** using all singular values (top) and the 20 first (bottom)

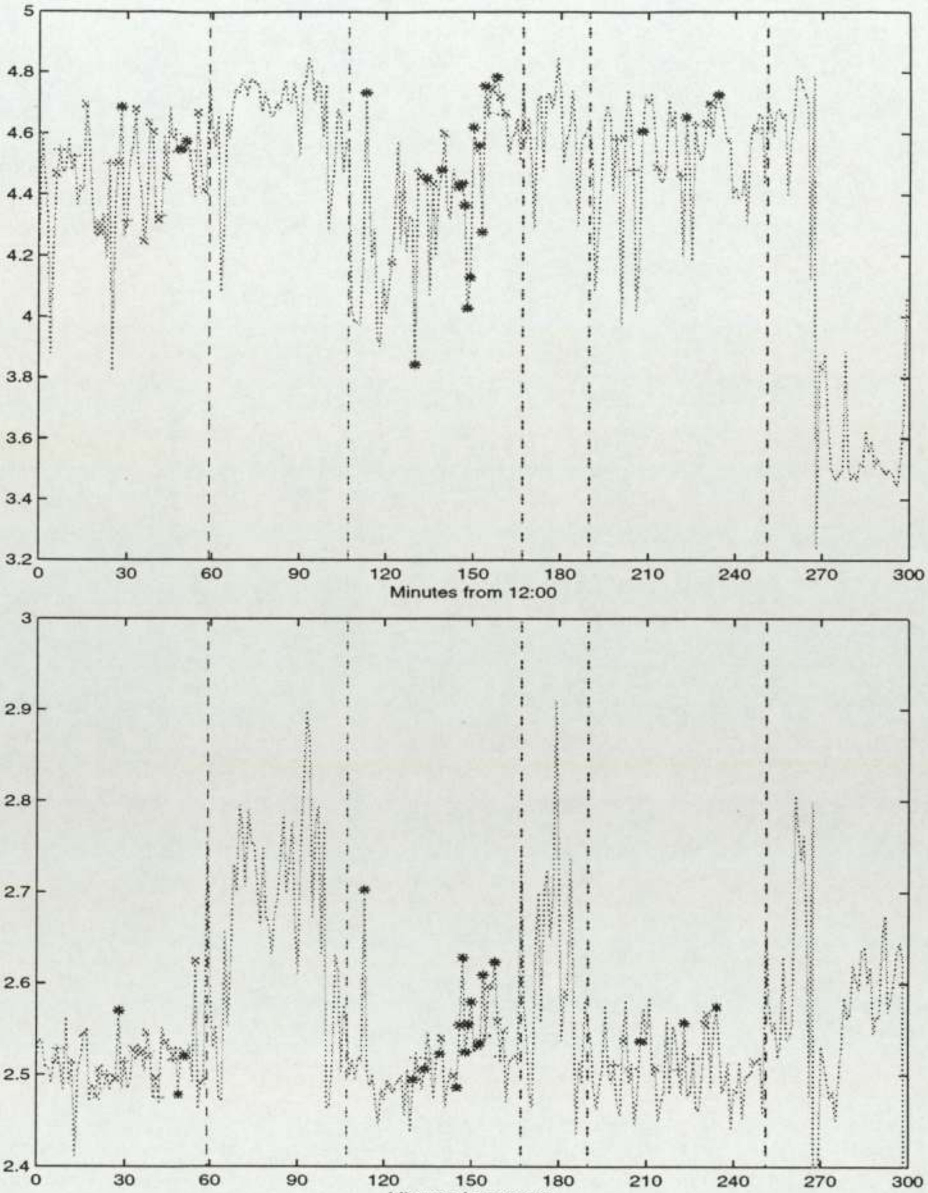

Figure B.7: **Entropy measures for channel P4:** using all singular values (top) and the 20 first values (bottom)

B.4 Fisher based measure applied to other channels

In this section, we present the results of the measure based on the Fisher's Information when applied to channel O2 (on this page) or to channel P4 (next page).

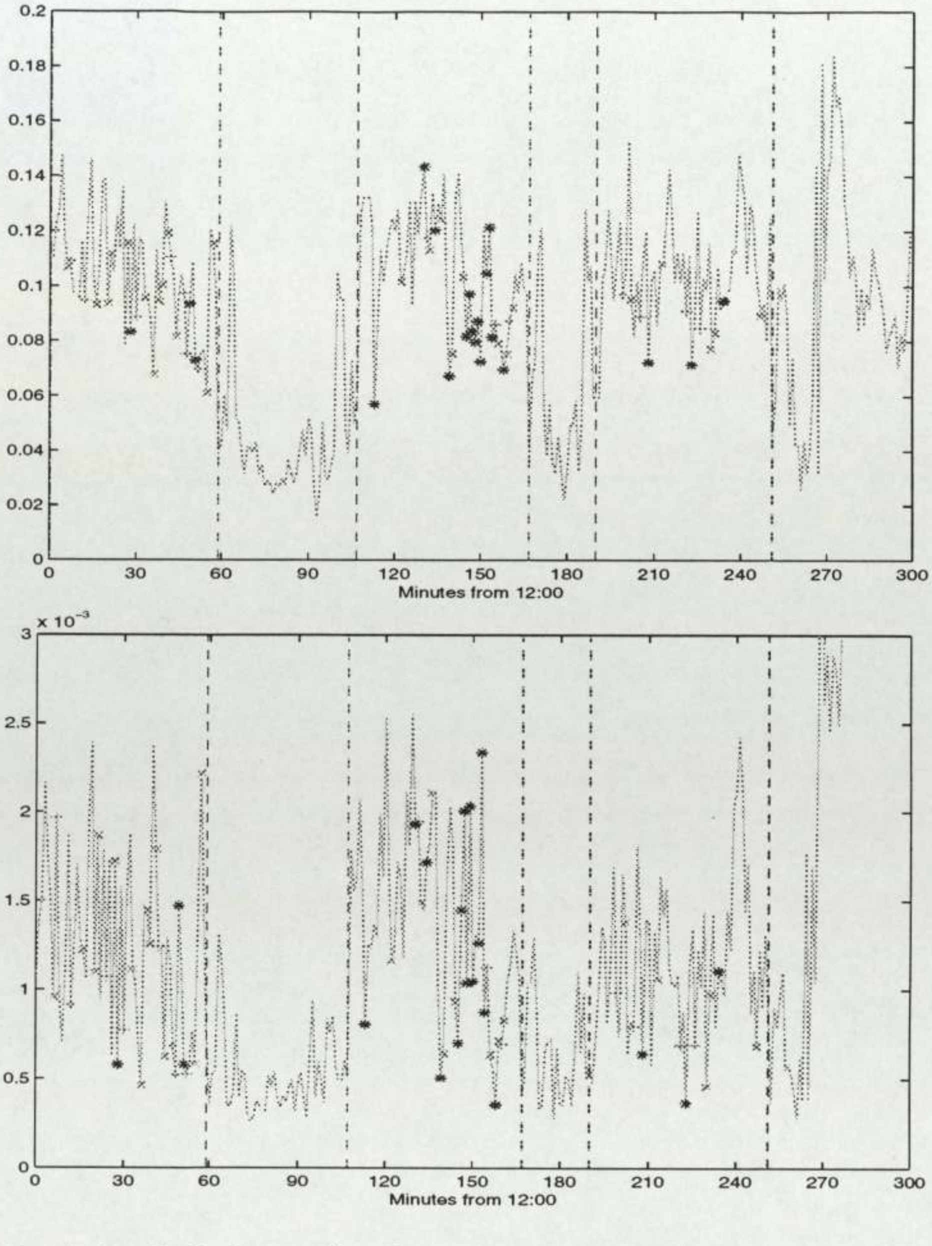

Figure B.8: **Fisher's Information based measures for channel O2:** using all singular values (top) and excluding the 5 first values (bottom)

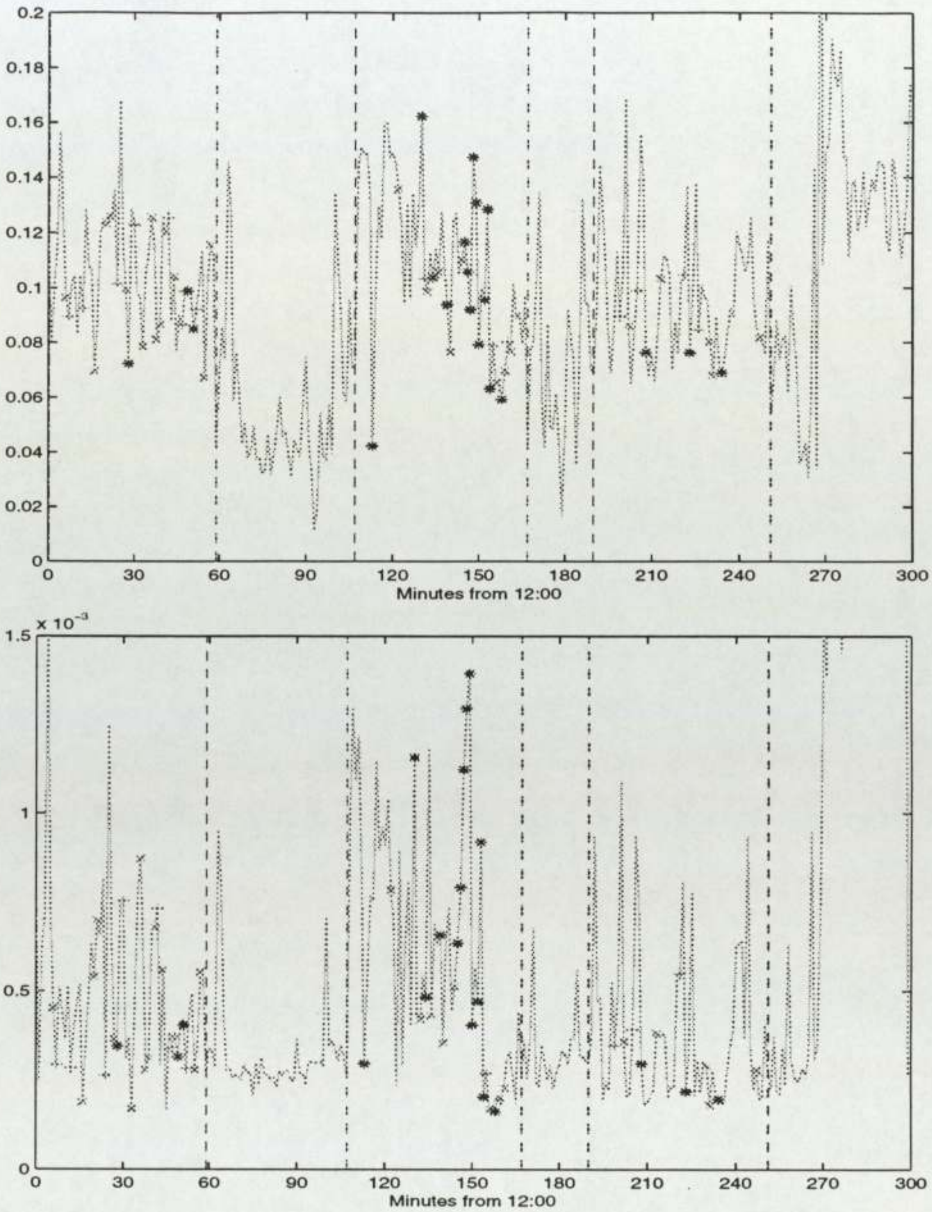

Figure B.9: **Fisher's Information based measures for channel P4:** using all singular values (top) and excluding the 5 first values (bottom)